THE JOURNAL OF PHYSICAL CHEMISTRY C
A JOURNAL OF THE AMERICAN CHEMICAL SOCIETY

pubs.acs.org/JPCC

Review Article

A Review on Lithium Phosphorus Oxynitride

Jed D. LaCoste, Andriy Zakutayev, and Ling Fei*

Cite This: https://dx.doi.org/10.1021/acs.jpcc.0c10001

Read Online

ACCESS | Metrics & More | Article Recommendations

ABSTRACT: Lithium phosphorus oxynitride (LiPON) has paved the way for thin film solid-state battery technology development and has shown application in a large range of fields since its first reported synthesis in 1993. The term LiPON describes the family of materials with the general formula of $Li_xPO_yN_z$ offering a great range of stoichiometries with varying properties. Understanding how the properties of LiPON are affected by different preparation methods is important for tuning this material to fit the required application. It is also useful to understand the LiPON relation between the amorphous structure and ionic conductivity, as well as the electrochemically degradation in contact with electrode materials. This review summarizes various methods of synthesizing LiPON and evaluates them on the basis of multiple properties of the resulting material. Structure−property relationships are identified to categorize the various LiPON stoichiometries that have been synthesized. Possible lithium ion conduction pathways and electrochemical degradation mechanism in LiPON are discussed. Representative applications of LiPON films are also introduced. At the end of this review, insights for future research into LiPON materials are provided.

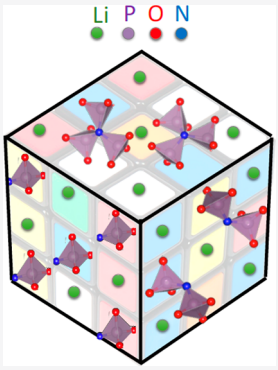

1. INTRODUCTION

Invention and commercialization of lithium ion batteries in 1980s powered a revolution in consumer electronics and energy technologies, ranging from small devices such as laptops, cellphones, and wearable electronics, to larger scale systems such as electric vehicles to solar energy storage.[1−3] Over the years, lithium ion batteries (LIBs) have become one of the most important energy storage technologies of modern society, as was recently celebrated by the 2019 Noble Prize in chemistry. However, traditional LIBs technology relies heavily on the use of highly flammable organic solvents as the transport medium for lithium ions, resulting in potential safety issues. These concerns may be mitigated using Li ion solid-state electrolytes,[4−7] which date back to 1960s,[8,9] yet remain a relatively new field of study for Li battery technology.[10]

Lithium phosphorus oxynitride (LiPON) has helped the way to solid-state lithium batteries, since its synthesis in early 1990s at Oak Ridge National Laboratories,[11,12] for primary use in thin film batteries. Literature reported values of LiPON's ionic conductivity range from 10^{-8} to 10^{-6} S/cm.[13] The mechanical properties of LiPON feature a shear modulus of 77 GPa, a value over 19 times that of lithium metal, proposed to enhance dendrite protection in LIBs with Li metal anodes.[14] As a result, LiPON has been the center of attention for safer lithium battery technology with high energy and power densities enabled by Li metal anodes. For example, LiPON has been successfully used as an electrolyte for lithium batteries with planar geometries and also showed great promise for lithium batteries with in 3D structured electrolytes.[15,16] Furthermore, LiPON has been applied in other technologies, such as electrochromic materials, microelectromechanical systems (MEMS), and wireless sensors.[17−20]

The term LiPON describes the family of compounds with a chemical formula of $Li_xPO_yN_z$, allowing for many different stoichiometries to be studied. This large number of possible stoichiometries allows for fine-tuning LiPON synthesis and structure to achieve high ionic conductivities and great mechanical properties. Both amorphous and crystalline LiPON materials have been achieved, and each show distinct properties depending on the synthesis method.[14,21−25] As summarized in Table 1, LiPON materials with a wide range of properties have been synthesized through a number of methods, including radio frequency magnetron sputtering, chemical vapor deposition (CVD), atomic layer deposition (ALD), pulsed laser deposition (PLD), solid-state reactions, and others.[11,15,19,24−30] Despite its importance for solid-state electrolytes, there are no reviews dedicated to LiPON, though several reviews on solid electrolytes include LiPON as a part of the discussion.[5,10,31,32] Thus, it is of great interest to have a focused review of different LiPON synthesis methods, stoichiometries and structures, and the corresponding properties. It is also great to note that a very recent noncrystalline solid-state electrolyte review paper has a large portion covering LiPON,[33] which offers some alternative

Received: November 5, 2020
Revised: January 11, 2021

Table 1. Summary of Various Synthesis Methods and the Resulting LiPON Stoichiometries Synthesized

pros of svnthesis method	cons of synthesis method	LiPON stoichiometry	ionic conductivity (S/cm)[a]	activation energy (eV)	ref
		Radio Frequency Magnetron Sputtering			
·currently the most popular method to produce LiPON	·expensive	$Li_{3.1}PO_{3.8}N_{0.16}$	2.00×10^{-6}	0.57	7
·capibility for thin or thick films	·high vacuum required	$Li_{3.3}PO_{3.8}N_{0.22}$	2.40×10^{-6}	0.56	7
·high quality, conformal coatings achievable	·inert atmosphere required for synthesis	$Li_{2.9}PO_{3.3}\ N_{0.46}$	3.30×10^{-6}	0.54	7
·large range of stoichiometries by changing sputtering conditions	·poor coatings on complex 3D strucutres	$Li_{3.13}PO_{1.69}N_{1.39}$	4.90×10^{-6}	0.55	10
·deposition rate controlable down to the nanometer	·slow deposition rates	N/A	1.80×10^{-6}	0.43	13
·nontoxic precusor materials		$Li_{4.4}PO_{4.3}$	1.00×10^{-6}	0.64	19
·radio frequency prevents charge build up on the target		$Li_{4.0}PO_{3.9}N_{0.4}$	1.70×10^{-6}	0.62	19
		$Li_{3.7}PO_{3.4}N_{0.7}$	2.30×10^{-6}	0.6	19
		$Li_{3.5}PO_{3.2}N_{0.8}$	2.60×10^{-6}	0.59	19
		$Li_{3.4}PO_{3.1}N_{0.9}$	2.80×10^{-4}	0.58	19
		$Li_{3.2}PO_{3.0}N_{1.0}$	3.00×10^{-6}	0.57	19
		$Li_{2.9}PO_{2.6}N_{0.91}$	2.10×10^{-6}	0.52	22
		$Li_{1.8}PO_{1.2}N_{1.5}$	1.70×10^{-6}	0.49	22
		$Li_{3.3}PO_{2.9}N_{0.83}$	3.10×10^{-6}	0.47	22
		$Li_{2.9}PO_{1.875}N_{1.25O}$	1.67×10^{-6}	0.492	29
		$Li_{2.410}PO_{2.651}N_{0.909}$	6.20×10^{-7}	0.499	29
		$Li_{2.795}PO_{2.670}N_{0.750}$	7.46×10^{-7}	0.551	29
		$Li_{2.708}PO_{2.920}N_{0.420}$	2.83×10^{-7}	0.551	29
		$Li_{2.852}PO_{2.931}N_{0.400}$	2.10×10^{-6}	0.594	29
		$Li_{3.4}PO_{4.5}N_{0.4}$	N/A	N/A	30
		$Li_{1.9}PO_{3.9}N_{0.7}$	N/A	N/A	30
		$Li_{1.4}PO_{3.9}N_{0.5}$	N/A	N/A	30
		$Li_{2.637}PO_{2.810}N_{0.325}$	8.95×10^{-7}	N/A	33
		$Li_{3.056}PO_{3.293}N_{0.221}$	1.85×10^{-8}	N/A	33
		$Li_{3.493}PO_{3.641}N_{0.107}$	7.35×10^{-9}	N/A	33
		Pulsed Laser Deposition			
·high quality, conformal coatings achievable	·low ionic conductivity	Li_2PO_2N	1.50×10^{-8}	0.68	31
·direct transfer of target stoichiometry to the substrate possible	·slow deposition rates				
·deposition rate controlable down to the nanometer	·expensive				
·large range of stoichiometries possible	·vacuum required				
·nontoxic precusor materials					
		Metal−Organic Chemical Reaction			
·thickness controllable down to the nanometer	·toxic precursors	N/A	2.95×10^{-7}	1.06	8
·good quality films of LiPON	·less stoichiometry avalible	$Li_{1.47}PO_{2.88}N_{0.24}$[b]	1.02×10^{-6}	N/A	32
	·high temperatures required				
		Atomic Layer Deposition			
·LiPON synthesis controlable down to the atomic level	·toxic precursors	N/A	7.50×10^{-9}	N/A	14
·high quality, conformal cotaings achievable	·limited range of stoichiometries	$Li_{0.95}PO_{3.00}N_{0.60}$	6.60×10^{-7}	0.66	15
·complex 3D architectures attainable					
		Solid-State Reactions			
cheap and simple method to produce LiPON	·low ionic conductivity	Li_2PO_2N	8.80×10^{-7}	0.57	20
	·limited range of stoichiometries				
	·high temperatures required				
		Solution Processed LiPON			
·cheap and simple method to produce LiPON	·less versatile stoichiometric control	$(Li_2PO_2N)_n$	1.7×10^{-10} (at 80 °C)	N/A	35
	·low ionic conductivity				
	·time consusming, multistep process				

[a]Values reported for room temperature unless marked otherwise. [b]Stoichiometry deteremined from experimental data from source.

https://dx.doi.org/10.1021/acs.jpcc.0c10001
J. Phys. Chem. C XXXX, XXX, XXX−XXX

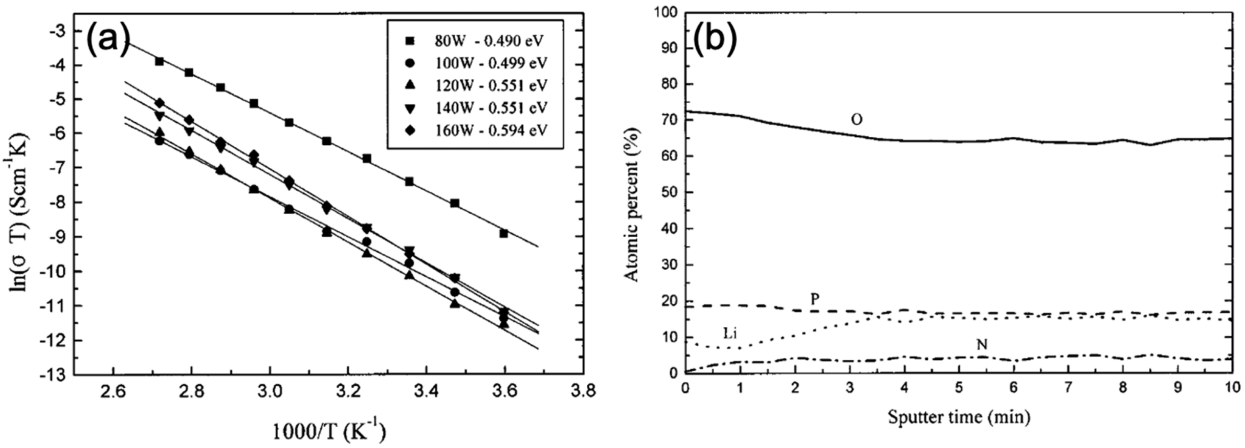

Figure 1. LiPON films deposited by RF sputtering. (a) Arrhenius plot of ionic conductivity of sputtered LiPON deposited at a RF power of 80−160 W vs temperature. The conductivity becomes lower and the slope becomes steeper as the sputtering power increases. (b) AES composition depth profile of LiPON. The chemical contents of the film do not change with the depth of the LiPON film. Reprinted with permission from ref 34. Copyright 2002 The Electrochemical Society.

perspectives on LiPON in addition to this LiPON exclusive review work.

In this review, various methods of synthesizing LiPON are summarized and evaluated on the basis of relevant properties of the resulting films. From the research findings of these different synthesis methods, structure−property relationships are evaluated to compare the various LiPON stoichiometries that have been synthesized over the past two decades. Possible lithium ion conduction mechanism and LiPON degradation pathways are summarized. Representative LIPON applications are also introduced, and insights for future research into LiPON materials are provided.

2. SYNTHETIC METHODS

2.1. Radio Frequency Magnetron Sputtering. Radio frequency (RF) magnetron sputtering of Li_3PO_4 in a nitrogen atmosphere is the original technique used to synthesize LiPON and is still, by far, the most common.[11] RF magnetron sputtering is a sputtering technique that uses a high-frequency alternating field to accelerate ionized argon, hitting a target made of the material to be sputtered and depositing the material on a substrate. During this process, argon does not react with the target material, reactive RF magnetron sputtering may be achieved through incorporation of a reactive gas such as nitrogen.[34] RF magnetron sputtering offers good quality films and can be scaled up, and thicknesses are controllable down to the nanometer level. On the other hand, this method is costly, requires vacuum technology, and offers low rates of deposition. However, RF magnetron sputtering allows for a simple synthesis that can easily be modified to adjust the stoichiometry of the resulting films allowing for more in-depth studies of the material over a large range of stoichiometries by adjusting power, gas pressure, and sputtering gases. In the sputtering of LiPON, Li_3PO_4 is usually used as target and pure nitrogen gas used as a reactive gas and in some cases, argon may be used as a carrier gas with nitrogen.[17,19,34,35] During the sputtering synthesis process of LiPON, three distinct reaction steps have been devised by Choi et al.:[34]

$$\text{Step 1: } N_2 \rightarrow 2N^+ + 2e^- \quad (1)$$

$$\text{Step 2: } Li_3PO_4 + xN^+ \rightarrow Li_3PO_{4-x}N_x \quad (2)$$

$$\begin{aligned} \text{Step 3: } & Li_3PO_{4-x}N_x \rightarrow Li_3PO_{4-x}N_x(\text{ads}) \\ & xO^+ + xe^- \rightarrow (1/2)O_2 \\ & (2-x)N^+ + (2-x)e^- \rightarrow (1/2)(2-x)N_2 \end{aligned} \quad (3)$$

Step one and step three are fast reactions, this is due to the high energy of the plasma in step one breaking nitrogen's bonds and the momentum of the particles in step three.[34] Step one shows the nitrogen gas being split into nitrogen ions and electrons, resulting in a reactive nitrogen cation species. Step two shows the incorporation of nitrogen ions into the lithium phosphate structure as a plasma. In step three, the nitrogen incorporated in the $Li_3PO_{4-x}N_x$ adsorbs to the substrate while oxygen removed from the lattice combines with electrons to produce diatomic oxygen. Finally, the excess nitrogen ions recombine with electrons to become electrically neutral.[34] Therefore, the rate limiting step is step two and is determined by the power applied to the target during sputtering.

Figure 1a shows the ionic conductivity of the LiPON films synthesized at various powers as a function of temperature. Fitting the data using the Arrhenius equation, it is found that the activation energies of the films increase with increasing power.[34] It is concluded in this study that the higher the power applied to the target, the lower the ionic conductivities and the higher the activation energies of the resulting LiPON. Figure 1b shows an Auger electron spectroscopy (AES) depth profile of LiPON. Throughout the sample, it is seen that the nitrogen content is uniform during the deposition. It is suggested that nitrogen incorporation in the LiPON is due to reactive sputtering and not due to poisoning of the target,[34] but we note that these two processes are intimately linked to each other. Furthermore, lower power sputtering results in higher ionic conductivity at the cost of stability. Cycling behavior is shown to become worse for the lower powered sputtering process due to the increase in diffusion range.[34] Developing the best performing LiPON electrolytes is a balancing act between high ionic conductivity and cycling stability, understanding the processes that affect these properties is important for further development of LiPON electrolytes.

2.2. Pulsed Laser Deposition. Pulsed laser deposition (PLD) is a synthesis method that uses a high-powered laser to

https://dx.doi.org/10.1021/acs.jpcc.0c10001
J. Phys. Chem. C XXXX, XXX, XXX−XXX

hit a target to be deposited on a substrate and offers its own advantages such as high deposition rates, easily controllable film thicknesses, and the ability to perform reactive/nonreactive depositions.[27,36] In PLD, a high-power pulsed laser is focused on the target material under a high vacuum; the pulsed laser vaporizes the target, which is then deposited on a substrate. In a study published in 2002, LiPON is prepared from a Li_3PO_4 target in a nitrogen atmosphere.[27] The first instance of LiPON produced through PLD shows characteristics very similar to those of LiPON produced through RF magnetron sputtering. Key parameters of the deposition process are explored, including nitrogen pressure and beam intensity. Results from this study show that increasing the nitrogen pressure decreases the film growth rate and improves the ionic conductivity through the incorporation of more nitrogen into the LiPON film; furthermore, increasing the laser power from 5 to 20 J/cm^2 shows an increase in ionic conductivity and film growth rate.[27]

Nonreactive deposition processes are of interest. Because in the absence of reactive gases, the stoichiometry of the target may be directly transferred to the substrate. This property is explored by the PLD of a Li_2PO_2N target synthesized through the solid-state reaction route. It is found that by using the crystalline LiPON target and depositing in a nitrogen atmosphere, the resulting thin film has a good ionic conductivity and an amorphous structure.[36] Further, the influence of the PLD-LiPON layer on the charge transfer resistance between amorphous LiPON and $LiMn_{1.485}Ni_{0.45}Cr_{0.05}O_4$ (LNM) cathode is explored. Findings from this study indicate that by depositing the amorphous PLD-LiPON between the LNM cathode and LiPON the charge transfer resistance is greatly reduced.[36] Reducing the charge transfer resistance between individual battery components is highly desired when developing solid-state batteries and is still an important issue to tackle. Having the ability to reduce resistances between LiPON and electrode materials by using another form of LiPON is an excellent solution to decreasing charge transfer resistances. It is theorized that this is due to the increase of nitrogen in the LiPON film by sputtering from a high nitrogen content target.[36] However, no conclusive explanation for the mechanism of this improvement is offered.

2.3. Metal−Organic Chemical Vapor Deposition. Metal−organic chemical vapor deposition (MOCVD) has also been successfully applied to synthesize LiPON through several reaction routes.[13,37] MOCVD uses vapor-phase precursors to deposit thin films of materials onto a substrate's surface. After the reactions are complete, the waste products are purged, and the film is collected. One possible route for LiPON from MOCVD is reacting lithium dipivaloylmethane (Li(DPM)), triethyl phosphate (TEP), and ammonia. Shown in Figure 2 is the reactor schematic for this process. Nitrogen gas is used as the inert gas for carrying Li(DPM) and TEP individually through heated lines into the reactor vessel (Figure 2). During this process, Li(DPM) is thermally degraded, requiring a Li^+ acceptor.[13] When TEP is decomposed, two distinct decomposition routes are seen; the first is where $-O-C_2H_5$ forms $-OH$ and C_2H_4, and the second is where $-OH$ and $-C_2H_5$ form $-C_2H_5OH$.[13] Ionic bonds form between the Li^+ from the Li(DMP) decomposition and the oxygen sites from the TEP decomposition; this reaction occurs at 500 °C.[13] Ammonia, incidentally decomposing at >500 °C, is introduced into the reactor to incorporate nitrogen into the film, producing LiPON. The growth rate increases monotonically up to 575 °C, as shown in Figure 3a.[13]

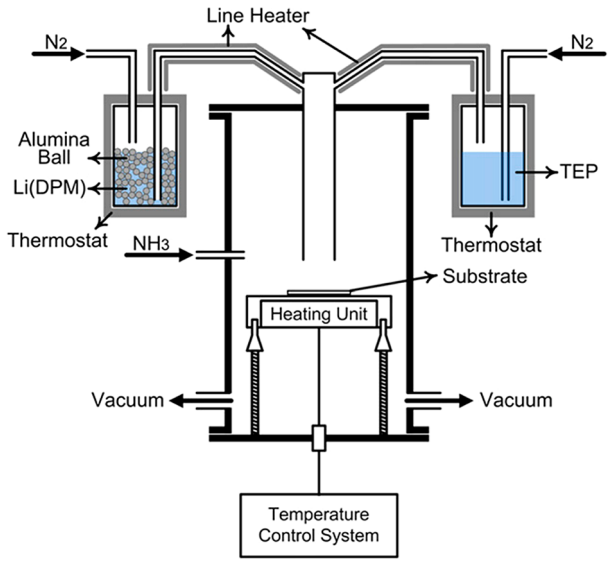

Figure 2. Schematic diagram of experimental setup for LiPON thin film deposition using MOCVD. Reprinted with permission from ref 13. Copyright 2013 Elsevier.

Figure 3b shows the temperature dependence of ionic conductivity of the LiPON film, it is seen that the ionic conductivity improves at higher reaction temperatures. Shown in Figure 3c is the ratio of triply coordinated to doubly coordinated nitrogen as a function of temperature. It can be seen that a higher amount of triply coordinated nitrogen is incorporated at higher temperatures, resulting in higher ionic conductivities. At 550 and 575 °C ionic conductivities for the LiPON range from 2.75×10^{-7} to 2.95×10^{-7} S/cm^{-1}, this is within the reported literature values for LiPON; however, on the low end, possibly due to adduct materials formed.[13]

Precursors of LiO^tBu and triethyl phosphate are also used to synthesize LiPON in an $Ar-H_2-N_2$ plasma assisted CVD process in the 2012 study by Maxie et al.[37] Deposition in an $Ar-O_2-N_2$ atmosphere is also investigated. Plasma enhanced chemical vapor deposition allows for LiPON deposition at lower temperatures and offers a higher rate of deposition. Results of this study show ionic conductivity consistent with typical LiPON and offer a higher growth rate compared to RF magnetron sputtering from Li_3PO_4. Furthermore, preparation in an $Ar-N_2-H_2$ atmosphere yields an ionic conductivity much higher than in the $Ar-N_2-O_2$ atmosphere.[37] A lower ionic conductivity for synthesis in the presence of oxygen indicates that the presence of oxygen may reduce the mobility of the lithium ions in the LiPON matrix.

2.4. Atomic Layer Deposition. Atomic layer deposition (ALD) is a method of synthesizing thin films that relies on the reactions of various precursors to build the desired structures layer-by-layer. Because of the ability to grown films in a stepwise fashion, more complex geometries can be prepared than by RF magnetron sputtering; this is especially important for the development of 3D architectures in lithium batteries.[15,16] ALD was first used to prepare LiPON in 2015, two different groups published their work on ALD of LiPON each using different precursors and reaction routes.[15,16]

In the first reported synthesis of LiPON through ALD, lithium *tert*-butoxide (LiO^tBu), H_2O, trimethyl phosphate (TMP), and N_2 are reacted in subsequent steps on silicon to grow LiPON thin films.[15] The schematic for this process can be seen in Figure

https://dx.doi.org/10.1021/acs.jpcc.0c10001
J. Phys. Chem. C XXXX, XXX, XXX−XXX

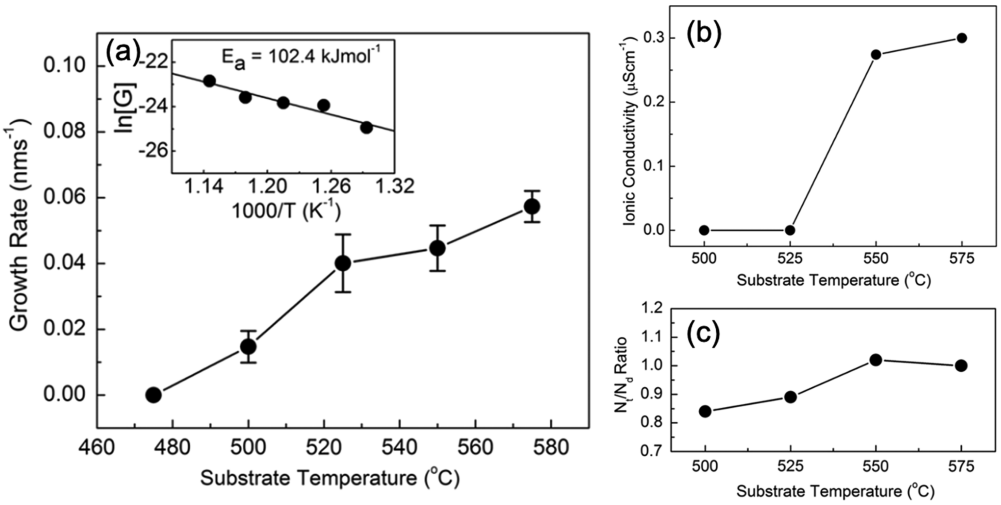

Figure 3. MOCVD of LiPON thin films. (a) Growth rate of LiPON films as a function of substrate temperature and Arrhenius plot for the growth rate (inset). (b) Li ion ionic conductivity of LiPON films as a function of substrate temperature (measurement temperature = 25 °C). (c) Ratio tripled coordinated nitrogen (P—N<P; N_t) to doubly coordinated nitrogen (P—N═P, N_d) as a function of substrate temperature. Reprinted with permission from ref 13. Copyright 2003 Elsevier.

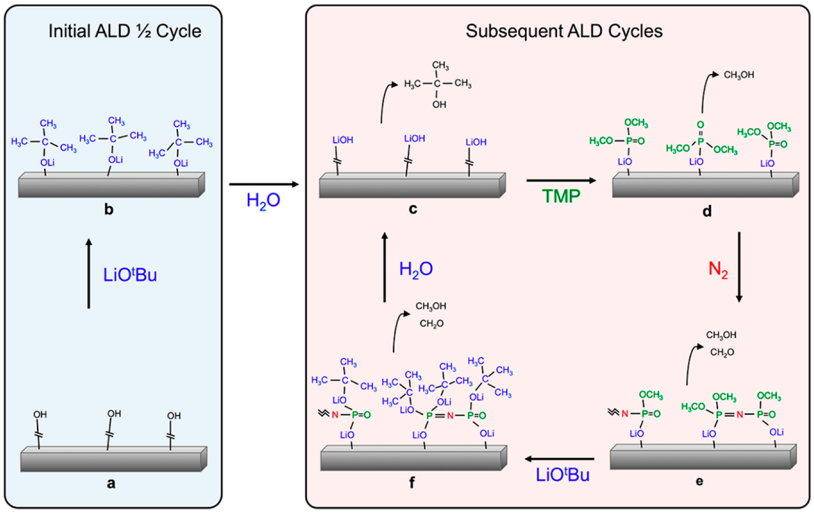

Figure 4. ALD growth mechanism of LiPON films. (a) The hydroxyl terminated substrate is shown. (b) The metastable surface after the LiO^{t}Bu pulse is shown. (c) The H_2O pulse removes the *tert*-butanol ligands and forms LiOH on the surface. (d) TMP reacts with surface LiOH through ligand exchange reaction, evolving CH_3OH. (e) N_2 plasma cross-links phosphorus atoms and evolves CH_3OH and CH_2O. (f) LiO^{t}Bu reacts with $-OCH_3$ ligands and evolves both CH_2OH and CH_2O. The initial LiOtBu and H_2O pulses shown in (a) and (b) are required to "activate" the substrate prior to deposition. For all subsequent ALD cycles, the process chemistry in (c) through (f) is repeated as one ALD cycle. Reprinted with permission from ref 15. Copyright 2015 American Chemical Society.

4. In the first step, a hydroxyl terminated substrate is reacted with LiO^{t}Bu, resulting in a metastable surface. H_2O is then reacted with this intermediate resulting in a LiOH surface and removing the *tert*-butanol ligand. Next, TMP is reacted with the LiOH through ligand exchange, releasing MeOH. Nitrogen plasma is then introduced to cross-link the phosphorus groups, evolving MeOH and CH_2O. Finally, LiO^{t}Bu is reacted with the $-OCH_3$ ligand, then MeOH and CH_2O are evolved, and H_2O is flushed through generating a LiOH surface. From this point, the cycle may be repeated until the desired film thickness is reached. This method yields various concentrations of nitrogen in the film by varied nitrogen pulse times, allowing for precise control of the nitrogen content, as determined by X-ray photoelectron spectroscopy (XPS). Nitrogen contents ranging from 0% to 16.3% are achieved through this method; however, it is noted that the resulting films offer lower ionic conductivities (1.45×10^{-7} S/cm), an order of magnitude lower compared to the best films from RF magnetron sputtering.[15]

In another work, ALD is also used to synthesize LiPON in a water free, binary process involving lithium hexamethyldisilizide ($LiN(SiMe)_3$(LiHMDS) and diethylphosphoramidate $(H_2NP(O))(OC_2H_5)_2$ with nitrogen as a carrier and purge gas. The feasibility of 3D structured systems is also assessed through depositing the LiPON on a 3D-microstructured silicon and is depicted in Figure 5. Results from these tests show that the LiPON layer is uniform in thickness from the top to the bottom of the trench, perfectly replicating the nanoscale roughness of the silicon substrate.[16] Similarly to the other LiPON produced from ALD, lower ionic conductivity values are seen with this process when compared to RF magnetron sputtered thin films of LiPON.[23,26,27,38] One suggestion for this is that the LiPON resulting from ALD has a more ordered

https://dx.doi.org/10.1021/acs.jpcc.0c10001
J. Phys. Chem. C XXXX, XXX, XXX−XXX

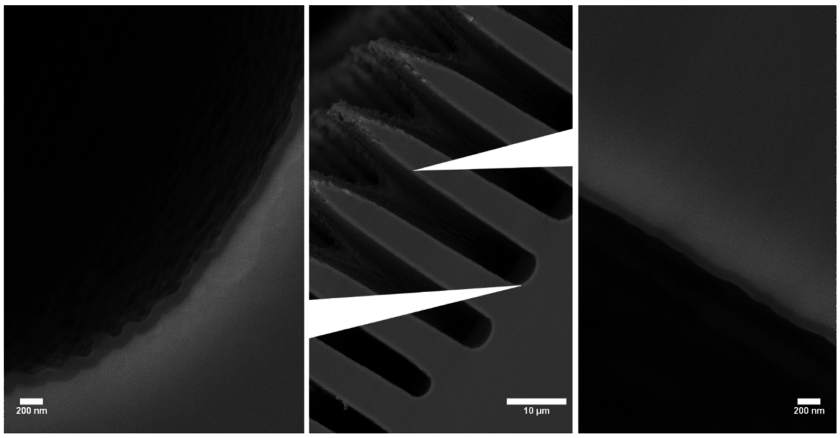

Figure 5. Cross-section SEM images of LiPON deposited by ALD on 3D-microstructured silicon. Reprinted with permission from ref 16. Copyright 2015 American Chemical Society.

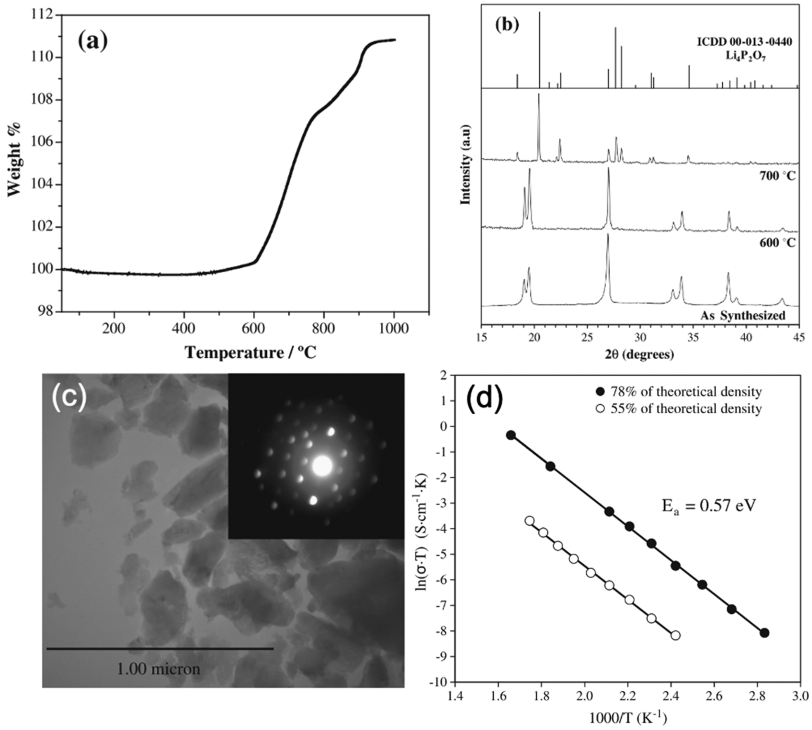

Figure 6. Bulk solid-state synthesis of LiPON. (a) The TGA curve after heating to 1000 °C in air and (b) XRD patterns of SD-Li_2PO_2N heated in air at 600 and 700 °C compared with the room temperature "as synthesized" pattern. The reference XRD pattern of the $Li_4P_2O_7$ decomposition material is shown in the top panel. (c) Representative TEM micrograph and electron diffraction pattern (inset) of SD-Li_2PO_2N acquired in bright field mode. (d) Arrhenius plot of measured impedance for SD-Li_2PO_2N for pellets with 55% and 78% of the theoretical density. Reprinted with permission from ref 24. Copyright 2013 Elsevier.

structure as an inherent feature of the deposition process. With other processes, such as RF magnetron sputtering, there is a more random nature to the particle collisions, resulting in a more amorphous LiPON. It is also worth mentioning that NaPON (sodium phosphorus oxynitride), inspired by and analogous to LiPON, recently was successfully prepared *via* a thermal ALD process, as the first sodium ion conductor synthesized by ALD.[39] Ultimately, ALD offers more versatility for electrolyte geometry compared to sputtering processes since the layers are built in subsequent steps and can be a great way to design electrolyte systems for 3D batteries in particular.

2.5. Solid-State Reactions. LiPON can be synthesized from a plethora of methods; however, it is uncommon to see crystalline LiPON. Solid-state reactions allow for the synthesis of these crystalline LiPON stoichiometries. Solid-state reaction routes are perhaps the least used method for synthesis of LiPON, the first reported solid-state synthesis of LiPON is in 1995 from Bate's group.[40] This work also reports the first synthesis of crystalline LiPON, although it is noted that another group also made claims of a Li_3PON_2 material but supplied no diffraction data to back their claims.[40] During the initial attempts, Li_2O and P_3N_5 are used as precursor materials and resulted in multiple phases. Li_3N and $LiPO_3$ are found to produce a single-phase material. Preparation of the LiPON through solid-state reaction is done by thoroughly crushing the precursors in an agate mortar, packed in a reaction vessel under

https://dx.doi.org/10.1021/acs.jpcc.0c10001
J. Phys. Chem. C XXXX, XXX, XXX−XXX

nitrogen, and then heated to 600 °C for 24 h. From this work, $Li_{2.88}PO_{3.73}N_{0.14}$ is reported as a polycrystalline sample and has a structure similar to γ-Li_3PO_4 with much higher ionic conductivity and lower activation energies due to Li ion and anion site vacancies.[40] Since there are a large number of stoichiometries for LiPON, there is still room for improvement on ionic conductivity of crystalline LiPON by modifying the preparation method.

In the 2012 study, Senevirathne et al. explored the synthesis of crystalline Li_2PO_2N from Li_2O, P_2O_5, and P_3N_5. In this work, the precursors are ground together in a mortar, compressed into a pellet, and then sintered under a vacuum at 950 °C for 10 h.[24] The resulting LiPON is shown to have a strong −P−N−P−N− backbone that is stabilized, retaining this stability up to 1050 °C *in vacuo* and 600 °C in air, as shown in Figure 6a.[24] Further, Figure 6b shows the change in the X-ray diffraction (XRD) pattern for the as-synthesized LiPON and after heating to 600 and 700 °C. Results from this data indicate that the as-synthesized LiPON decomposes into a $Li_4P_2O_7$ structure.[24] Transmission electron microscopy (TEM) images and electron diffraction (inset) (Figure 6c) show this synthesis produces irregular discrete crystalline particles instead of a film. Further, the ionic conductivity, shown in Figure 6d, is evaluated for samples that are at 55% and 78% the theoretical density of SD-Li_2PO_2N (the name refers to their experimentally obtained compound), revealing high ionic conductivity at higher density. These findings hold important implications for the development of LiPON based technology applications in high temperature environments because the LiPON particles do not degrade at 600 °C.

2.6. Solution-Processed LiPON. Wet chemical methods for LiPON synthesis are currently at the infancy stage. Recently, in an effort to prepare LiPON from wet chemical methods, polymeric LiPON has been synthesized from a modified polyphosphazine synthesis route.[41] Synthesis of LiPON from wet chemical methods is very attractive for large scale manufacturing, as all of the current industrial methods for LiPON synthesis require vacuum technology and as a result thicker films are more costly.

Figure 7 shows the reaction steps for the one-pot synthesis of polymeric LiPON. Step 1 shows the polymerization of poly(dichlorophosphazene) from lithium bis(trimethylsilyl)-amide) ($LiN(SiMe_3)_2$), phosphorus trichloride (PCl_3), phosphorus pentachloride (PCl_5), and thionyl chloride (SO_2Cl_2). In step 2, dimethyl sulfoxide (DMSO) is added to the dried reaction product from step 1 and then reacted for 48 h at 40 °C, forming the reaction product of poly(phosphoramidic acid). Finally, in the third step of the reactions sequence, poly-(phosphoramidic acid) is reacted with *n*-butyllithium in toluene for 96 h under stirring to produce polymeric LiPON. The overall yield of polymeric LiPON is 58% on the basis of $(NPCl_2)_n$.[41] Polymeric LiPON prepared through this reaction route shows excellent solubility in toluene and tetrahydrofuran with no indications of cross-linking.[41] Solubility of the polymeric LiPON in these solvents clearly distinguishes the polymeric LiPON from LiPON prepared from other methods and has profound implications regarding processability and industrial scale up. However, the ionic conductivity of the polymeric LiPON is determined to be 1.7×10^{-10} S/cm, which is much lower than LiPON produced from any other methods.[41] It is noted that reaction between LiPON and lithium metal forms a stable interface of high conducting reactants such as Li_3N and Li_3P and this may be beneficial and a possible way to improve the performance *in situ*.[25,41] Exploration of wet chemistry methods to synthesize LiPON shows great promise for the development of future of LiPON based technologies.

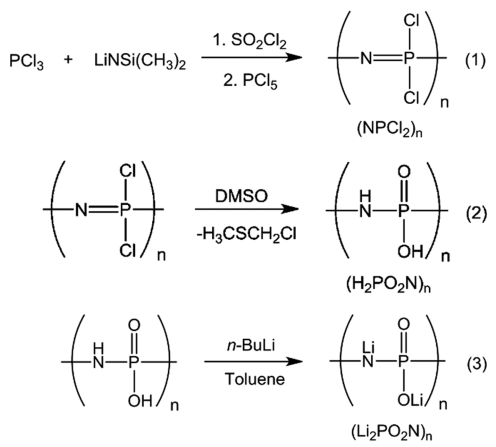

Figure 7. Reaction scheme for synthesis of polymeric LiPON. Reprinted with permission from ref 41. Copyright 2020 Elsevier.

3. STRUCTURE−PROPERTY RELATIONSHIPS

Elucidating the structure of amorphous materials is difficult, making developing structure−property relationships arduous. There have been no conclusive explanations for the excellent electrochemical properties of LiPON; however, it is a general consensus that the incorporation of nitrogen is responsible for the properties of LiPON. In the original work regarding LiPON, it is explained that the incorporation of nitrogen creates −N═ and −N< bonds with phosphorus, where −N< is referred to as a "cross-linked" structure and is said to be the reason for the high ionic conductivity.[11] In later years the scientific community, in agreement with this theory, began referring to −N═ and −N< as doubly (N_d) and triply (N_t) coordinated nitrogen, respectively. Further, in Mascaraque's work on interpreting the ionic conductivity increase related to nitrogen, a relationship between the triply coordinated nitrogen and doubly coordinated nitrogen in a LiPON film is suggested. The relationships between the number of N_t, N_d, bridging oxygens (BO), and nonbridging oxygens (NBO) is described by the following equations:[42]

$$N_t = \frac{3}{2}BO$$

$$N_d = 1NBO + \frac{1}{2}BO$$

This theory of LiPON structure containing N_d and N_t configurations has been accepted by the scientific community since it was suggested, in recent years more insight into the structure of amorphous LiPON has been achieved.

In 2018, the amorphous structure of LiPON is resolved by Dudney's team utilizing both theoretical calculations and experimental data. Results of this study suggests that nitrogen exists as apical nitrogen (N_a) in isolated $P(O,N)_4$ tetrahedra as well as bridges between two phosphate groups (N_b).[43] Figure 8 shows a schematic of the simulated $Li_{2.9}PO_{3.5}N_{0.31}$ with the presence of apical nitrogen and doubly coordinated nitrogen. These results agree with literature in that there are two distinct nitrogen arrangements in LiPON; however, this work suggests a perhaps better description of the nitrogen binding arrange-

https://dx.doi.org/10.1021/acs.jpcc.0c10001
J. Phys. Chem. C XXXX, XXX, XXX−XXX

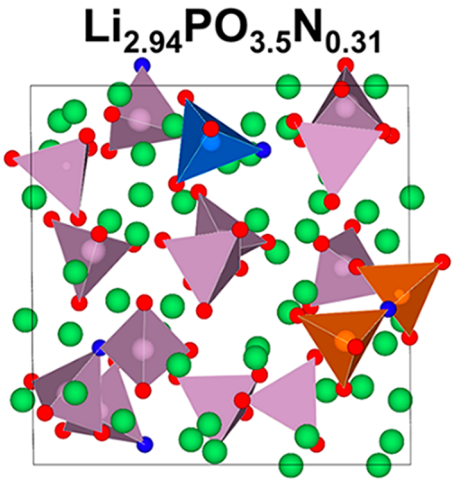

Figure 8. Schematic of simulated $Li_{2.94}PO_{3.50}N_{0.31}$ structure from ab initio molecular dynamics. Red atoms are O, blue atoms are N, green atoms are Li, and light gray atoms are P. The triangles are added to outline the phosphate tetrahedra. Reprinted with permission from ref 43. Copyright 2018 American Chemical Society.

ments. It is further suggested that triply coordinated nitrogen (−N<) may exist, although neutron pair distribution functions along with spectral data back up the simulated data show no triply coordinated nitrogen.[43] Validating this work, *ab initio* molecular dynamic simulations are employed and show the lack of triply coordinated nitrogen groups and presence of both apical and double bridging nitrogen.[25] Three possible spatial configurations of nitrogen in LiPON are summarized in Figure 9: apical, double, and triple coordination. It is worth noting that

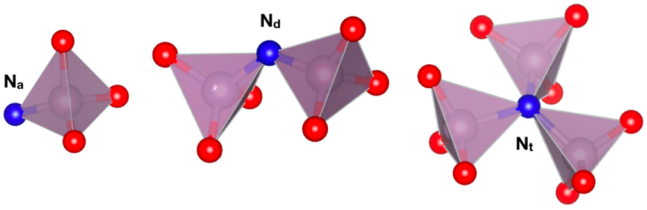

Figure 9. Schematic representation of the possible N configurations in phosphate structures: apical N (N_a), double bridging N (N_d), and triple bridging N (N_t). Color code: N (blue), P (gray), O (red). Reprinted with permission from ref 25. Copyright 2018 American Chemical Society.

a similar amorphous glassy material, lithium boron oxynitride (LiBON) only contains N−B−N bridges between two triangular boron subunits.[44] Also like LiPON, the suggestion for improvements in ionic conductivity is due to the nitrogen causing decreased local interactions between Li^+ within the matrix. Shown in Figure 10a, the ionic conductivity of LiPON is represented as a function of Li:P ratio and further shows the distinction between apical, double bridges, and triple bridged nitrogen. Figure 10b shows a phase diagram relating the phosphate group arrangements to the ionic conductivity. Evaluation of these figures hints that the presence of triply coordinated nitrogen primarily exists in the meta- and pyrophosphate arrangements. Relating these features to crystallinity indicates that the presence of triply coordinated nitrogen may be more dominant in the more crystalline LiPON stoichiometries. Further, it is suggested that the conductivity trends of LiPON are associated with the amorphousness, excess of Li, and structural changes. Higher degrees of amorphous character yield higher ionic conductivities, as the triply coordinated nitrogen may slow lithium ion transport. This indicates that the presence of the triply coordinated nitrogen creates a more crystalline material resulting in lower ionic conductivity. Orientational disordering of the phosphate polyhedral in amorphous LiPON creates edge sharing between LiO_4 and PO_4 tetrahedra as well as under- and overcoordinated lithium sites, increasing the energy of the lithium sites.[25] This increase in the energy of the lithium sites is attributed to the increase in mobility of lithium particles in the amorphous matrix. Increasing the Li−Li interactions caused by the excessive lithium from the (N^{3-}:O^{2-}) 1:1 substitution, and the increase in density caused by the bridging (N_b), further increases the lithium site energy.[25] Furthermore, the nitrogen bridging condensation of the phosphate units lowers the electrostatic interaction between Li^+ and anions.[25] By decreasing the interaction between lithium ions and the anions, the ionic conductivity is improved. It is seen that the incorporation of the nitrogen groups into the ceramic electrolyte allows for the improvement in ionic conductivity for the amorphous LiPON, the presence of oxygen in the matrix decreases ionic conductivity due to the stronger interactions with lithium ions. Annealing LiPON films has also been shown to be affective in improving the ionic conductivity. When LiPON is annealed at 100, 200, 300, and 400 °C, the resistivity is tracked and shows a minimal resistivity at 200 °C with an increase in resistivity after.[21] This change in ionic conductivity is shown to be a function of the Li/P ratio, shown in Table 2 are the tabulated data from these experiments. Table 2 shows that at higher Li/P ratios, the resistivity of the LiPON film is improved; this indicates that lithium ion mobility is highest when Li/P is high.

Stoichiometric ratios between each element in the LiPON matrix play an important role in the resulting properties of the film. One of the most important ratios is the N/P ratio, increasing this value has been shown to improve the ionic conductivity of the LiPON thin films.[23] Understanding how the N/P ratio changes with respect to Li/P and O/P are important factors to consider for elucidating the reaction details. It has been shown that there is a linear dependence of oxygen to nitrogen where 1.3 oxygens are replaced by 1.0 nitrogen; this processes correlates to a loss of one lithium.[23] This is consistent with the findings from the reaction mechanism in the study from Choi et al. and show that ionic conductivity increases with an increasing N/P ratio (decreasing Li/P ratio), suggesting the improvement in ionic conductivity is a result of the incorporation of nitrogen to the lithium phosphate matrix.[34]

The local structure of amorphous LiPON is further resolved *via* a combined experimental and computational approach, showing the prevalence of Q^0_0 PO_4^{3-} tetrahedra and identifying N incorporation to form dimeric units *via* bridging N and separately nonbridging N on orthophosphate tetrahedra.[45] The high stability of LiPON is described structurally as a combination of the low connectivity of the structure as well as the hyper-annealing that occurs with physical vapor deposition. Free-standing and flexible LiPON film was also successfully prepared in this work, which is a great progress in LiPON synthesis.

4. LITHIUM ION CONDUCTION IN LIPON

As mentioned in the previous section, many researchers, by varying experimental design combinations, have come to realize critical factors that affecting LiPON ionic conductivity such as

https://dx.doi.org/10.1021/acs.jpcc.0c10001
J. Phys. Chem. C XXXX, XXX, XXX−XXX

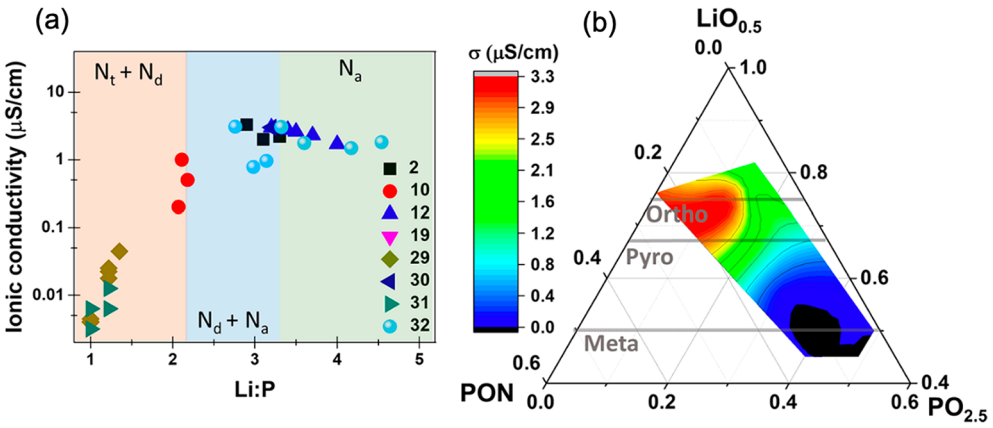

Figure 10. (a) Measured ionic conductivity of LiPON as a function of Li content at room temperature. The legend highlights the literature used to extract the data (the citations listed are from the source paper). (b) Calculated ternary diagram showing the ionic conductivity vs the composition. Reprinted with permission from ref 43. Copyright 2018 American Chemical Society.

Table 2. Literature Reported Values of Resistivity and Li 1s/P 2p Ratio at Variable Annealing Temperatures[a]

T (°C)	impedance (Ω)	Li ls/P 2p
25 (as deposited)	37.87	7.04
100	36	9.52
200	28.62	10.27
300	37.79	5.88
400	269992	3.92

[a]Reprinted with permission from ref 21. Copyright 2020 Elsevier.

the amount of nitrogen incorporation into the glass structure and the ratio of apical, doubly, and triply coordinated nitrogen. However, few works are available on elucidating Li ion motion or the conduction mechanisms in LiPON. Because the vast number of stoichiometries and the complexity of amorphous phases makes the analysis very challenging, thanks to the advancement of computer simulation and machine learning, scientists now could conduct both experiments and calculations with synthesized LiPON films and cross-verify the results, making it easier to reveal more information in great depth of amorphous materials.[25,43,46,47] As such, the physical chemistry aspects of LiPON can be potentially best understood through a combination of experiments and computational techniques.

Van-Jodin et al. investigated the dielectric properties, conductivity, and Li^+ ion motion in LiPON thin films prepared by RF magnetron sputtering. In their work, LiPON

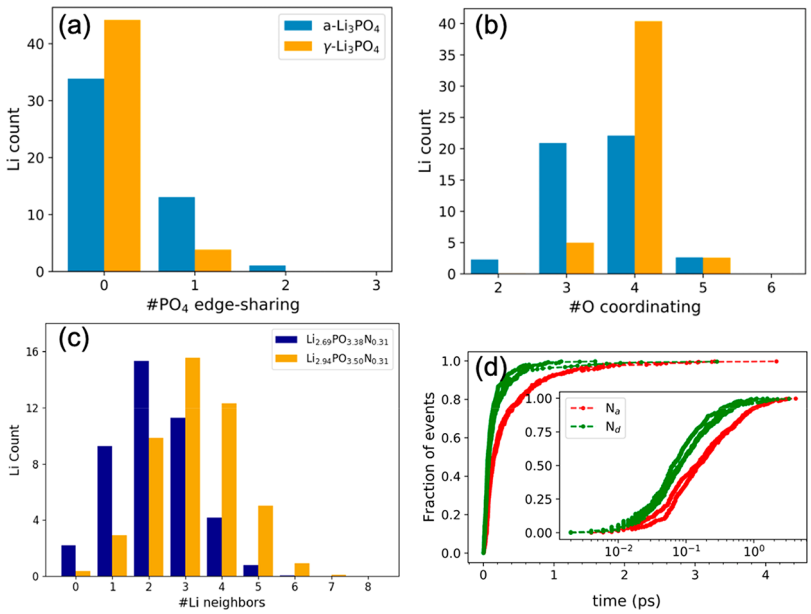

Figure 11. Statistical averages calculated from molecular dynamics for a-Li_3PO_4 and a-$Li_{3.25}PO_4$ over 10 ps long sample trajectories at 1000 K. Panel a shows the average amount of LiO_4−PO_4 edge-sharing within a maximum Li−P distance of 2.7 Å. Panel b displays the average number of O coordinating Li within a distance of 2.5 Å. Panel c shows the average Li−Li neighbors density distributions calculated for LiPON structure models of compositions $Li_{2.69}PO_{3.38}N_{0.31}$ and $Li_{2.94}PO_{3.50}N_{0.31}$, over 10 ps long sample trajectories at 1000 K. Li neighbors were selected within a sphere of radius 3.0 Å around each Li. (d) Fraction of events happening around N and O atoms in $Li_{2.94}PO_{3.50}N_{0.31}$, during a simulation time of 30 ps at 1000 K (semilogarithmic plot in the inset). An event is defined as one Li ion entering a sphere of radius r = 2.5 Å (sphere of influence) around the atom. The bottom right panel compares different types of N: there are 2 N_a and 3 N_d species in the structure, represented in red and green, respectively. Reprinted with permission from ref 25. Copyright 2018 American Chemical Society.

https://dx.doi.org/10.1021/acs.jpcc.0c10001
J. Phys. Chem. C XXXX, XXX, XXX−XXX

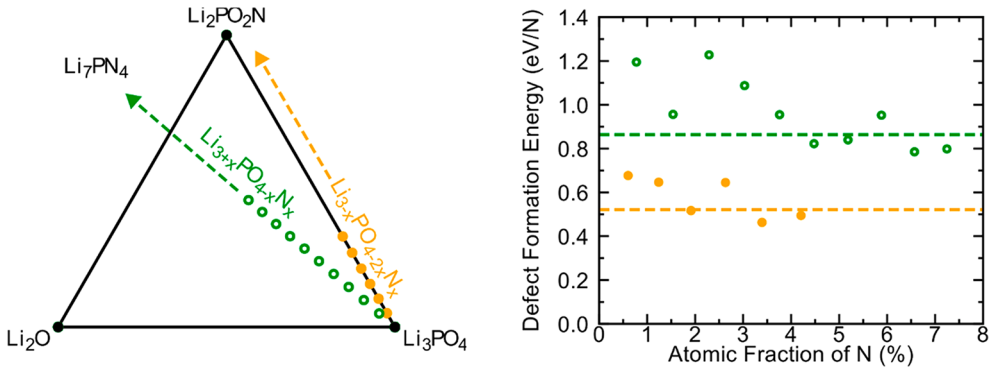

Figure 12. DFT phase diagram for LiPON near-ground-state crystal structures with N_a (green points) and N_d (orange points) defects as identified with the GA-MLP method. All defected structures lie above the hull; i.e., they are thermodynamically unstable and eventually decompose favored with respect to N_a defects. Defect formation energies corresponding to such decompositions are plotted in the right panel, showing that N_d defects are energetically favored. Reprinted with permission from ref 25. Copyright 2018 American Chemical Society.

composition, ionic conductivity, and electronic conductivity are measured experimentally.[48] While charge carrier concentration, mobility and Li ion diffusion coefficients are concluded by calculation. The influence of temperature (80−380 K) on the conductivity and permittivity properties of LiPON and the time dependence of current under an electrical field are also analyzed in great detail. Transport properties are then correlated with an analysis of the chemical composition. It is concluded that the transport mechanism in LiPON occurs mainly by hopping with only one kind of carrier that has a fixed concentration regardless of the temperature. Therefore, the increase of ionic conductivity is only due to the increase of mobility, as the activation energy of the mobility remains almost the same. Quantitatively, only 4% of Li ions are involved in the conduction process. To facilitate the mobility of ions, a slight expansion of the material without modification of the ions' local surrounding can be created.[48] The results of this work agrees well with the conclusion drawn by Fleutot et al. For example, they also confirmed by NMR measurements that only a part of lithium from LiPON is involved in the conductivity.[23]

Optimization of solid electrolyte design for applications in solid-state batteries is an important area of research. A 3D model is suggested to model the lithium ion conductivity due to the nonlinear conduction pathways.[49] The conductivity of LiPON is suggested to depend heavily on temperature and film thicknesses. In detail, the thickness of the film controls the Li^+ concentration at constant flux and lower temperature operation shows an increase in the Li^+ mobility due to the electrostatic interactions between Li^+ reducing, allowing for a directional flux of Li^+. It also suggests a LiPON film with a thickness smaller than 10 nm would provide the highest conductivity. These findings can potentially guide the design LiPON films for low- and high-temperature battery applications.

From computational studies, atomistic-level insight into the mechanisms of Li ion mobility ascribed to the chemistry and connectivity of the phosphate polyanions near Li^+ in amorphous LiPON has been gained by researchers.[25] Evaluation of Li ion mobility is completed through *ab initio* molecular dynamics (AIMD) simulations. First, property variances between γ-Li_3PO_4 and amorphous Li_3PO_4(a-Li_3PO_4) are evaluated, as Li_3PO_4 is commonly used as starting raw material for LiPON synthesis. Second, nitrogen incorporation into the a-Li_3PO_4 was assessed by varying the nitrogen content to investigate the potential condensation between phosphate units as well as lithium ion deficiencies or excess.[25] The relative defect formation energies were also evaluated to offer insight into the effects of N on the coordination environment, uncovering the influences on stoichiometry. Figure 11 shows a summary of the data from this work. Panels a and b of Figure 11 show calculations for Li_3PO_4 that determine the edge sharing and oxygen coordination with Li. In Figure 11c, the neighboring Li−Li density distributions are determined to elucidate the local Li−Li interactions in representative LiPON. Mechanistically, the formation of N_a and N_d defects are described by two routes. N_a is formed by the substitution (N^{3-} + Li^+) ↔ O^{2-}, leaving the (O+N):P ratio at a constant 4:1 and with excess Li^+ along the binary Li_3PO_4−Li_7PN_4.[25] N_d defects are formed through the substitution N^{3-} ↔ ($2O^2$ + Li^+), generating deficiencies in Li and anion content with respect to Li_3PO_4, forming one and three-dimensional double bridging condensates of Li_2PNO_2 and $LiPN_2$.[25] Figure 12 shows the DFT phase diagram for LiPON near the ground-state crystal structure and the corresponding traces for N_a and N_d formation (green and orange respectively), as well as the average defect formation energies for N_d and N_a, found to be around 0.5 and 0.9 eV, respectively. In highly energetic synthesis processes, the formation of N_a and N_d are both equally likely; Figure 11d shows the frequencies of N_a and N_d occurrences, indicating the likelihood of both N_a and N_d formation. In comparison to amorphous and crystalline Li_3PO_4, LiPON is placed into an interesting class of ion conductors where conductivity increases with density, going against the idea that a larger volume with more "open space" improves conductivity, as seen in Li_3PO_4.[25]

In short, it is determined that the several factors that contribute to enhanced lithium ion mobility, and therefore allow for ionic conductivity optimization in LiPON, are orientation disordering of PO_4 polyhedra creating LiO_4−PO_4 edge sharing, increased Li−Li interactions from the 1:1 N:O substitution and densification from N, and the lowering of electrostatic interaction between Li^+ and the anions due to N-bridging.[25] Maximizing Li ion mobility in LiPON relies on the accommodation of N_d bridges while accommodating a high concentration of charge carriers, implying excess Li and isolated O should be minimized. Suggesting a relatively comprehensive mechanism of conductivity in LiPON, this work represents a great step toward elucidating the structural and composition aspects of LiPON that govern lithium ion conduction.

https://dx.doi.org/10.1021/acs.jpcc.0c10001
J. Phys. Chem. C XXXX, XXX, XXX−XXX

5. ELECTROCHEMICAL DEGRADATION OF LIPON

As LiPON has been widely applied in electrochemical devices as a solid-state electrolyte or buffer layer to protect electrode materials, understanding how the chemistry of LiPON changes under the influence of an applied field and the interface reaction/stabilization processes of LiPON with cathode/lithium represents an important area of research. In 2018, Put et al. studied LiPON electrochemistry and decomposition chemistry through a combination of computational and experimental methods, contributing to a detailed understanding of the voltage effect and thus the electric field over LiPON.[50] In the experiment, LiPON is placed between TiN and Au, and then a positive or negative potential bias is applied for observation. Under the influence of a positive bias, the lithium ions diffuse toward the TiN blocking electrode and create an enhanced double layer that keeps the electric field localized at the interfaces. Since TiN does not alloy or intercalate with lithium, lithium ions will be reduced to metallic filaments that shortcircuits the layer under a high enough potential. In return, Joule heating or electromigration resulting from the large currents from the short circuits can destroy part of the filament; LiPON decomposition occurs when the decomposition potential threshold (4.3−4.5 V) is met, releasing Li ions from the layer while creating phosphorus rich components of $Li_4P_2O_7$, $LiPO_3$, and finally P_4O_{10}, as well as generating oxygen and nitrogen gas. The Cottrell equation fitting reveals that the decomposition happens in a diffusion limited way. It also suggests the mobile lithium ions in the material are able to keep the electric field located at the interface even at high potentials. Conversely, when a negative bias is applied, the lithium ions diffuse toward the Au electrode. Formation of an Au/Li alloy occurs when the bias exceeds the decomposition voltage (4.3−4.5 V) and later lithium plating happens until all of the lithium is depleted from the LiPON layer, forming P_4O_{10}. The Au electrode is considered as a lithium sink that promotes dielectric breakdown of the remaining phosphate material, resulting in the eventual breakdown of the layer.

Electrochemical breakdown is irreversible and causes permanent damage to the LiPON electrolyte. Furthermore, another extremely crucial governing factor of LiPON breakdown is the time allowed for lithium depletion, occurring through the formation of a percolative pathway. A summary of the different reactions and their associated potentials that can occur on application of a bias to the LiPON layer and the different breakdown models is presented in Figure 13.[50] Noteworthy, the LiPON decomposition potential found in this work is very close to the decomposition potential range of 4.1−4.25 V calculated by both Richards et al. and Zhu et al.[51,52]

The property of the electrode−electrolyte interface is very critical for the performance of electrochemical devices (e.g., all-solid battery cells). Wang et al. utilized in situ STEM-EELS analysis to investigate the interlayer formation and evolution in a $LiCoO_2$/LiPON/Si thin film battery. It is uncovered that a structurally disordered interfacial layer between the $LiCoO_2$ cathode and LiPON electrolyte inherently exists without cycling. Upon *in situ* charging, this interfacial layer showed profound reactivity and evolved to form highly oxidized Co ionic species along with lithium oxide and lithium peroxide species, suggesting the interfacial impedance at the $LiCoO_2$/LiPON interface is caused by chemical changes rather than space charge effects.[53] Understanding the role of interfaces in solid-state batteries is necessary to improve the current state of the art. A

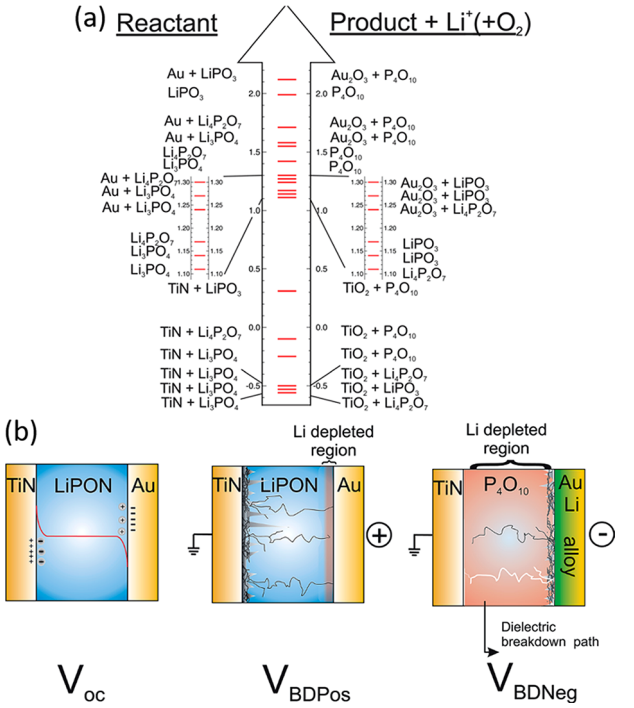

Figure 13. (a) Overview of the different reactions and their associated potentials (in V) that can occur on application of a bias to the LiPO(N) layer. The left side of the graph shows the species involved in the reaction; the right side shows the resulting products. All of the reactions lead to the generation of xe^{-1}, xLi^+, and possibly O_2 (not shown on this graph). (b) Schematic illustration of different breakdown modes for a LiPON layer sandwiched between gold and TiN electrodes. V_{OC} shows the structure without a bias application, V_{BDPos} shows the breakdown after application of a positive bias, and V_{BDNeg} depicts the structure after breakdown under negative sweep direction. Eventually hard breakdown occurs through the formation of a percolative defect path. Reprinted with permission from ref 50. Copyright 2018 Royal Society of Chemistry.

semiquantitative method combining scanning transmission electron microscopy with electron energy loss spectroscopy (STEM/EELS) reports precise mapping of the interfaces within nanobatteries.[54]

In the work completed by Fingerle et al. the stability of the LiPON and $LiCoO_2$ interface was evaluated both computationally and experimentally. They further investigated the annealing effect on the formation and evolution of $LiCoO_2$−LiPON interfaces to identify interlayer compounds related to the deposition process and to study the reactions and interlayer formation at the $LiCoO_2$−LiPON interface. Results show that the LiPON layer sputtered on $LiCoO_2$ exhibits secondary structures such as $LiNO_2$ formed on the $LiCoO_2$ surface. During low temperature annealing, the $LiNO_2$ disappears. When the process temperature is increased, a transformation of the LiPON network first occurs. During the formation of this interface, an electrostatic potential gradient is formed and is retained even after annealing. Upon annealing, the high temperature reactions form Co_3O_4 and degrade the LiPON network.[55] Photoelectron spectroscopy was also applied to probe the interfacial structure of LiPON/$LiCoO_2$; it is found that an intermediate layer composed of new species that differs in its chemical composition from the cathode as well as the LiPON solid electrolyte material and changes with growing layer thickness is formed, further supporting that an interfacial reaction between LiPON/$LiCoO_2$

https://dx.doi.org/10.1021/acs.jpcc.0c10001
J. Phys. Chem. C XXXX, XXX, XXX−XXX

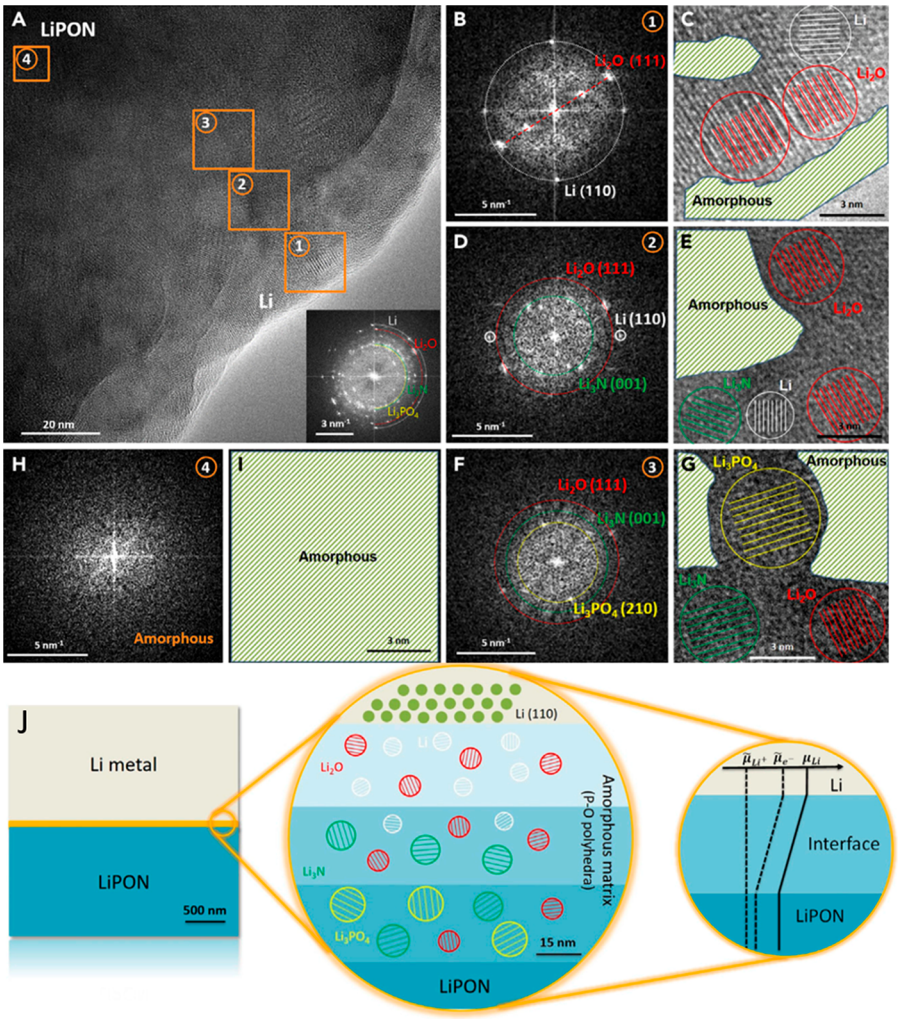

Figure 14. (A) HRTEM image of the interphase where four regions (regions 1−4) are highlighted by orange squares to indicate different stages of the multilayered structure across the interphase. The inset image is the FFT result of the whole area in (A). (B, D, F, and H) FFT patterns corresponding to regions 1−4 as highlighted in (A), respectively. (C, E, G, and I) Nanostructure schematic overlaying the HRTEM images that correspond to regions 1−4 as highlighted in (A), respectively. (J) Li/LiPON multilayered interphase schematic. Reprinted with permission from ref 65. Copyright 2020 Elsevier.

exists.[56] Electronic structure DFT calculations were also performed to predict interfacial degradation reactions of crystalline LiPON with Li_xCoO_2 and lithium electrodes. Results of this study suggest that LiPON models with purely P−N−P backbones are kinetically inert toward lithium at room temperature. In contrast, oxygen atoms transfer much faster from low-energy Li_xCoO_2(104) surfaces to LiPON under ambient conditions. It is also concluded that O atoms added to the crystalline LiPON interior remain mobile, which potentially creates pathways for further degradation of Li_xCoO_2 during battery cycling.[57] Note that this work assumes that interfacial reactions on amorphous and crystalline LiPON models are similar, which could lead to some level of deviation from experimental results.

The stability of LiPON films with lithium has remained a hot point for discussion and research as inconsistent results are reported by different groups. The general consensus is that LiPON does not react with lithium metal, and the reported values of electrochemical stability window for LiPON are up to 5.5 V (vs Li/Li+).[11,14,19,24,27,28,34,38,43,58−62] Recently, however, an *in situ* XPS study on the stability of the LiPON/lithium interfaces reveals that there are reactions that occur between LiPON and lithium metal. Results of this study show that exposure to metallic lithium breaks down the LiPON into smaller species such as Li_3PO_4, Li_3P, Li_3N, and Li_2O, leading to the disruption of the network structure of the LiPON glass.[30] Further analysis indicates that the LiPON/lithium interface stabilizes after the formation of a passivation layer, stopping the reactions. The species formed, such as Li_3N and Li_3P have ionic conductivities on the order of 10^{-4} and 10^{-3} S/cm, respectively, values much higher than LiPON's reported values.[63,64] This property of LiPON to form a high ionic conductivity passivation layer against lithium metal shows great promise for relieving the stability issues associated with long-term contact with lithium metal, while offering excellent lithium ion transport. The in situ XPS results was further supported by a qualitative and quantitative study enabled by cryogenic focused ion beam (cryo-FIB) and cryogenic electron microscopy (cryo-EM), which have the capability to preserve and probe samples for quantitative structural and chemical analysis.[65] In this recent study, cryo-FIB and cryo-EM were coupled to realize the morphology and chemical analysis of the interphase between LiPON and lithium metal. The interphase is found to be a multilayer-mosaic solid electrolyte interphase (SEI) structure

https://dx.doi.org/10.1021/acs.jpcc.0c10001
J. Phys. Chem. C XXXX, XXX, XXX−XXX

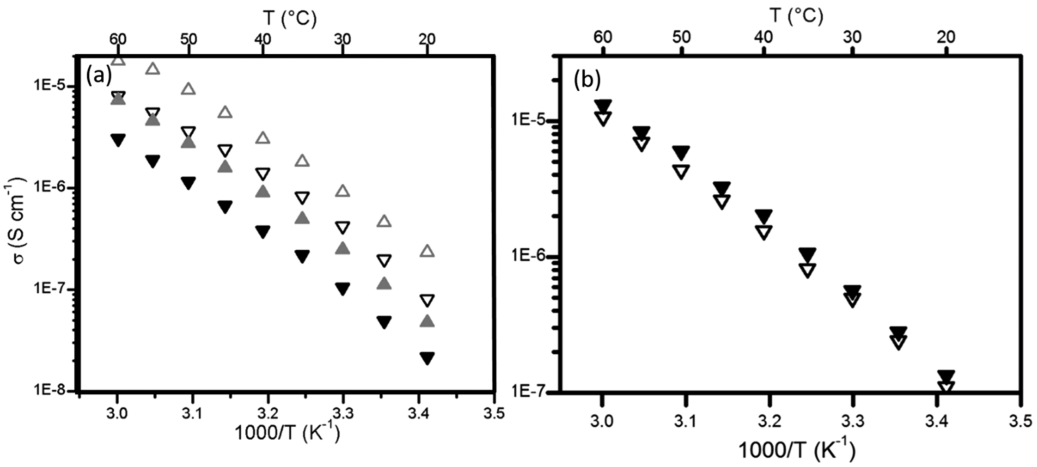

Figure 15. Experimentally measured (closed symbols) and calculated (open symbols) temperature dependence of conductivity for PMMA-EO/LiPON and PS-EO/LiPON. (b) Experimental (closed symbols) and calculated (open symbols) temperature dependence of the bilayer's conductivity for LiPON on PMMA-EO. Reprinted with permission from ref 74. Copyright 2011 The Electrochemical Society.

with concentration gradients of nitrogen and phosphorus and consist a distribution of crystalline decomposition products embedded within an amorphous matrix. As shown in Figure 14A-I, the observed structural and chemical evolution across the interphase identifies the SEI components to be Li_2O, Li_3N, and Li_3PO4, confirmed by XPS depth profiling. For a more straightforward conclusion, the schematic illustration of the interface is shown in Figure 14J. The composition and the mosaic formation are consistent with previous report.[30,66] Some SEM imaging observations of the interface changes between LiPON and lithium foil are also provided by Yoon's groups.[67]

In addition to the interface study of LiPON with lithium and $LiCoO_2$, other research such as the effect of atmospheric humidity on the chemical and microstructural changes of LiPON, lithium dendrite formation on LiPON, and solid−liquid electrolyte interphase formation on LiPON thin films are also available, providing valuable information for LiPON handing and the safety of LiPON based batteries.[68−70] In short, the results from these studies are important for development of LiPON based devices, as understanding how charge transfer and electrode chemistry affects the LiPON stoichiometry is crucial to minimize adverse effects. Further research into LiPON and electrode interfaces is still necessary due to the variety of LiPON stoichiometry and the lack of widely agreed rules or principles to guide the design and control of these reactive interfaces.

6. APPLICATIONS

Since its discovery, LiPON has been researched as a material for vastly different applications including lithium batteries, electrochromic devices, and dielectric materials. Versatility is one of the many appealing aspects that LiPON has to offer. LiPON has been successfully applied as a protective layer to solid electrolytes and electrode material in lithium batteries.[23,46,62] Currently, LiPON is used predominantly in thin film batteries[71] and has been shown to be an effective protective layer preventing dendrite penetration of the electrolyte when deposited on lithium metal.[72,73] Not only can LiPON offer a protective layer between a polymer electrolyte and lithium metal in a bilayered configuration, the structural integrity of the LiPON layer can be improved. For instance, when LiPON is deposited onto a nonrigid polymer substrate, mechanical stresses are relieved and the bilayer structure is preserved.[74] This property has profound implications on the use of LiPON as a protective layer for a higher conductivity polymer electrolyte, since the ionic conductivity of LiPON is typically too low for use in larger than thin film batteries. On the one hand, this study shows that laminating a polymer electrolyte allows for the synergistic combination of the solid polymer electrolyte (SPE) and the inorganic solid electrolyte (ISE). Conversely, by reversing the preparation method to deposit polymer electrolyte on a sputtered LiPON film, it is found that the resistivity increases substantially, as shown in Figure 15a,b.[74] LiPON has a high chemical resistivity allowing for longer contact time with lithium metal.[7,11,23,25,29,30,34,38,61,62,66,72,73,75,76,63,64,66−68] In our research, it is found that 30 nm of LiPON is the critical thickness for protecting a solid polymer electrolyte consisting of poly(propylene carbonate) and poly(ethylene oxide) in a bilayered electrolyte system.[66] It has also been shown that LiPON acts as a protective layer when sputtered onto a $La_{2/3-x}Li_{3x}TiO_3$ (LLTO) support, enhancing the chemical stability against lithium metal.[62]

In lithium ion batteries, lithium loss to the graphite containing electrode is one of the major causes of aging losses.[77] By engineering a surface to include an artificial solid electrolyte interface(SEI), the life of the cell is shown to be improved. LiPON is a suitable candidate for artificial SEI selection due to its relatively good stability and moderate ionic conductivity. In Liu's work, artificial SEI layers are deposited on Li-$Ni_{0.8}Co_{0.15}Al_{0.05}O_2$/graphite electrode in full cells. When LiPON is compared against the other artificial SEI layers, LiPON shows the best long-term stability as evidenced by capacity loss comparisons.[77] The results of this study are important for continued development of LiPON based batteries, even though the ionic conductivity may not be as high as more recent materials, the long-term stability and ability to deposit thin films of LiPON are quite appealing for improving long-term performance of current commercial cells.

In Li−S batteries, 250 nm coatings of LiPON on lithium metal anodes are shown to improve the overall performance of the cells.[73] When LiPON is deposited onto a lithium metal anode through plasma assisted deposition of e-beam reactive evaporation, the stability of the anode is improved greatly. When in contact with high concentrations of polysulfide solution for 60 days, it is shown that the LiPON is chemically stable, whereas SEI layers typically are etched by these types of

https://dx.doi.org/10.1021/acs.jpcc.0c10001
J. Phys. Chem. C XXXX, XXX, XXX−XXX

conditions, exposing lithium metal.[73] When introduced to a humid environment, the LiPON coated Li and the pure Li are shown to have noticeable differences. In a 40% relative humidity environment, lithium foil tarnishes almost immediately; when coated with 250 nm of LiPON, noticeable tarnishing occurs after 8 h.[73] Results from this study indicate that the stability of the lithium anode is improved in both atmospheric conditions and cell conditions. Overall, the LiPON coating is electrochemically stable and mechanically stable and offers a highly ionically conductive interfacial layer for the lithium metal anode in an Li–S battery.[73] Results from this study show great promise for the use of LiPON as an artificial SEI layer in Li–S battery chemistries, allowing for much more stable interfaces by minimizing the corrosive reactions typically seen by these types of cells.

When LiPON is coated on lithium metal in a Li(LiPON)/LAGP-PEO(LiTFSI)/$LiFePO_4$ full cell, similar improvements are noticed. Different thicknesses of LiPON on lithium metal are investigated to show a critical LiPON thickness of 500 nm.[72] The initial discharge capacity of 152.4 mAh g^{-1} for this full cell does not decay even after 150 cycles.[72] Results from this study further show that LiPON is a superior material for offering lithium metal anode protection in both solid-state cells and liquid electrolyte cells. Hindering the formation of dendrites improves the safety of the lithium cells even further for liquid electrolyte based batteries and offers an excellent solution to solid-state dendrite formation problem.

In an effort to suppress the degradation of the oxyfluoride electrode, LiPON has also been coated on FeOF type electrodes through atomic layer deposition. FeOF is an attractive electrode material because it offers high voltages of the fluorides FeF_x and the good kinetics of the oxides.[78] However, the first step in lithiation of FeOF results in the metastable $Li_nFeO_xF_{2-x}$, soon becoming unstable with a further increase in lithium ions in the FeOF formula unit.[78] Increasing the lithium content results in spontaneous decomposition into the rock-salt-phase LiFeO and the insulating LiF according the following reaction: $Li_nFeOF \rightarrow Li_{n-y}FeO + yLiF$.[78] It is found that, when LiPON is deposited on the FeOF electrode through atomic layer deposition, the conversion of lithiation products is suppressed. When a 30 nm LiPON layer is deposited on the FeOF based electrode, the performance of the cells was greatly improved, resulting in a capacity retention of ∼90% at 100 cycles.[78]

Beyond applications toward battery materials, LiPON has also been shown to be a suitable dielectric material. Fabrication of high-k dielectric materials is important in developing ultralarge scale integrated storage capacitors for dynamic random access memory technology.[76] Commonly, silicon dioxide is used in electronics, having a dielectric constant of 3.9; the dielectric constant for LiPON is determined to be 16.6 with a low leakage voltage.[76] These results are important for development of future memory storage technology where high-k dielectrics are needed, past the traditional dielectric SiO_2. With further advancement of LiPON, more applications will be enabled.

7. SUMMARY AND OUTLOOK

In this review, the recent progress in lithium phosphorus oxynitride synthesis *via* various routes has been summarized and discussed. For each route, the parameter control and LiPON synthesis mechanisms were introduced. Commentary on the advantages and disadvantages of various preparation routes was also provided. A summarizing LiPON properties *via* different methods was presented in Table 1. Due to the great versatility in LiPON characteristics such as stoichiometry and crystallinity, LiPON has shown different unique properties for applications in a variety of fields. A detailed discussion of the structure–property relationships is included in this review, leading into a detailed discussion of lithium ion mobility and LiPON breakdown chemistry. Along with this, applications of LiPON in multifarious fields are also introduced.

Currently, the most popular routes for LiPON synthesis utilize high-vacuum technology to grow thin films. With these types of methods, the cost is very high and the obtained LiPON material usually is in the limited form of a thin film. Very few reports on solid-state reaction routes prepare LiPON in bulk powder form, and the powders are difficult to produce conformal films. Further research to focus on wet chemistry methods of LiPON synthesis holds great promise for the development of LiPON based materials. Wet chemistry methods of LiPON synthesis offer better processability, scalability, and low-cost synthesis compared to routes that require vacuum synthesis or expensive equipment. In addition, it also has the versatility to produce LiPON in various forms. For example, LiPON produced from wet chemistry routes can produce films by various coating methods like dip or spin coating, be isolated as a powder, or be directly deposited on electrode materials as a protecting layer. Application of LiPON as a protective interface in solid-state batteries is a promising direction to improve the stability of electrode/electrolyte interfaces. Furthermore, additives can potentially be incorporated into the polymeric LiPON during production to improve ionic conductivity, allowing for more versatility.

In addition to LiPON synthesis, recent developments in computer simulations and experimental techniques can allow for the optimization of LiPON and offer great insight on where and how far the future research can go. Since LiPON has a multitude of different stoichiometries, computational methods can be greatly useful for predicting the different combinations of stoichiometries and the electrochemical properties. In detail, computer simulation and machine learning can predict and design LiPON optimized stoichiometry to achieve high ionic conductivity and allow for the specific control of other properties such as mechanical and electrical, which will greatly guide the experimentalists' work and significantly reduce time and cost. With laboratory work in combination with computational methods and molecular modeling, LiPON with new exceptional properties is also possible to be realized for an even wider range of applications. In conclusion, the comprehensive summary of current LiPON status and the insight for future research offered in this review can help the research community better understand this interesting material and further accelerate the development of LiPON for energy field and other innovative applications.

■ AUTHOR INFORMATION

Corresponding Author

Ling Fei – *Department of Chemical Engineering, Institute for Materials Research and Innovations, University of Louisiana at Lafayette, Lafayette, Louisiana 70504, United States;* orcid.org/0000-0002-0954-5168; Email: ling.fei@louisiana.edu

https://dx.doi.org/10.1021/acs.jpcc.0c10001
J. Phys. Chem. C XXXX, XXX, XXX–XXX

Authors

Jed D. LaCoste − *Department of Chemical Engineering, Institute for Materials Research and Innovations, University of Louisiana at Lafayette, Lafayette, Louisiana 70504, United States*

Andriy Zakutayev − *Materials Science Center, National Renewable Energy Laboratory, Golden, Colorado 80401, United States;* orcid.org/0000-0002-3054-5525

Complete contact information is available at: https://pubs.acs.org/10.1021/acs.jpcc.0c10001

Author Contributions

The manuscript was written through contributions of all authors. All authors have given approval to the final version of the manuscript.

Notes

The authors declare no competing financial interest.

Biographies

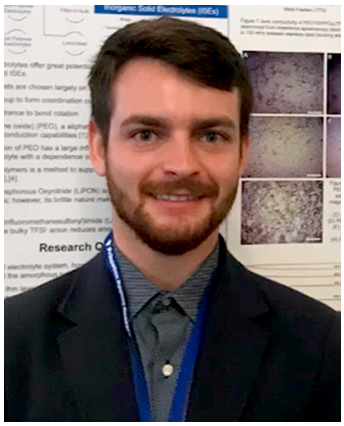

Jed D. LaCoste received his BS degree in Chemical Engineering from the University of Louisiana at Lafayette in 2018. He completed his master's degree under the supervision of Dr. Ling Fei in 2020. During his time as a master's student Jed has worked in collaboration with Dr. Andriy Zakutayev at the National Renewable Energy Laboratory on his thesis work regarding solid-state electrolytes for lithium batteries. His research interests include renewable energy, materials science, catalysis, electrochemical engineering, and surface science. Jed is currently attending Colorado School of Mines to work on his PhD in Chemical and Biological Engineering.

Andriy Zakutayev received his BS in Electronics from Lviv Polytechnic National University in 2006, and Ph.D. in Physics from Oregon State University in 2010. As a postdoc at National Renewable Energy Laboratory (NREL), he worked on designing new materials for photovoltaic solar cells, doing combinatorial experiments in collaboration with computational scientists. Currently Andriy is a scientist at NREL leading a team of researchers working on materials discovery for a wide range of energy technologies, including advanced anodes and solid electrolytes for Li ion batteries.

Ling Fei received her BS in Applied Chemistry from Shantou University in 2010 and PhD in Chemical Engineering from New Mexico State University in 2014. She served as a postdoc in the School of Chemical and Biomolecular Engineering at Cornell University from 2014 to 2016 and then worked as a Sr. Scientist in Axium Nano, LLC for one and a half year. She currently is an Assistant Professor in the Department of Chemical Engineering at The University of Louisiana at Lafayette. Her research focuses on the design, synthesis, and engineering of nanostructured materials for various applications including energy storage and conversion, surface coating, drug delivery, catalysis, and water purification.

ACKNOWLEDGMENTS

We acknowledge the financial support from National Science Foundation (NSF) under the award No. 1832963 and NSF(2020)-CIMM Seed Grant-37. L.F. also acknowledges Chevron Corporation for providing a Chevron Endowed Professorship in Chemical Engineering to support her research. Contribution from A.Z. was supported by the Laboratory Directed Research and Development (LDRD) Program at National Renewable Energy Laboratory (NREL), operated by Alliance for Sustainable Energy, LLC, for the U.S. Department of Energy (DOE) under Contract No. DE-AC36-08GO28308. The views expressed in the article do not necessarily represent the views of the DOE or the U.S. Government.

REFERENCES

(1) Nishi, Y. The Development of Lithium Ion Secondary Batteries. *Chem. Rec.* **2001**, *1* (5), 406−413.

(2) Yoshino, A. The Birth of the Lithium-Ion Battery. *Angew. Chem., Int. Ed.* **2012**, *51* (24), 5798−5800.

(3) Liu, W. Multilayer Composite Solid Electrolytes for Lithium Ion. *Dissertations*. ALL, 2016.

(4) Bachman, J. C.; Muy, S.; Grimaud, A.; Chang, H. H.; Pour, N.; Lux, S. F.; Paschos, O.; Maglia, F.; Lupart, S.; Lamp, P.; et al. Inorganic Solid-State Electrolytes for Lithium Batteries: Mechanisms and Properties Governing Ion Conduction. *Chem. Rev.* **2016**, *116* (1), 140−162.

(5) Kim, J. G.; Son, B.; Mukherjee, S.; Schuppert, N.; Bates, A.; Kwon, O.; Choi, M. J.; Chung, H. Y.; Park, S. A Review of Lithium and Non-Lithium Based Solid State Batteries. *J. Power Sources* **2015**, *282*, 299−322.

(6) Liu, Q.; Geng, Z.; Han, C.; Fu, Y.; Li, S.; He, Y. bing; Kang, F.; Li, B. Challenges and Perspectives of Garnet Solid Electrolytes for All Solid-State Lithium Batteries. *J. Power Sources* **2018**, *389*, 120−134.

(7) Chen, R.; Qu, W.; Guo, X.; Li, L.; Wu, F. The Pursuit of Solid-State Electrolytes for Lithium Batteries: From Comprehensive Insight to Emerging Horizons. *Mater. Horiz.* **2016**, *3*, 487−516.

(8) Liang, C. C.; Bro, P. A High-Voltage, Solid-State Battery System: I. Design Considerations. *J. Electrochem. Soc.* **1969**, *116*, 1322−1323.

(9) Liang, C. C.; Epstein, J.; Boyle, G. H. A High-Voltage, Solid-State Battery System II. Fabrication of Thin-Film Cells. *J. Electrochem. Soc.* **1969**, *116*, 1452−1454.

(10) Manthiram, A.; Yu, X.; Wang, S. Lithium Battery Chemistries Enabled by Solid-State Electrolytes. *Nat. Publ. Gr.* **2017**, *2*, 16103.

(11) Bates, J. B.; Dudney, N. J.; Gruzalski, G. R.; Zuhr, R. A.; Choudhury, A. Fabrication and Characterization of Amorphous Lithium Electrolyte Thin Films and Rechargeable Thin-Film Batteries. *J. Power Sources* **1993**, *43*, 103−110.

(12) Bates, J. B.; Dudney, N. J.; Gruzalski, G. R.; Zuhr, R. A.; Choudhury, A.; Luck, C. F.; Robertson, J. D. Electrical Properties of Amorphous Lithium Electrolyte Thin Films. *Solid State Ionics* **1992**, *53*−*56* (PART 1), 647−654.

(13) Tak, H.; Mun, T.; Park, C.; Wan, S.; Young, H. Characteristics of Lithium Phosphorous Oxynitride Thin Films Deposited by Metal-Organic Chemical Vapor Deposition Technique. *J. Power Sources* **2013**, *244*, 641−645.

(14) Herbert, E. G.; Tenhaeff, W. E.; Dudney, N. J.; Pharr, G. M. Mechanical Characterization of LiPON Films Using Nanoindentation. *Thin Solid Films* **2011**, *520*, 413−418.

(15) Kozen, A. C.; Pearse, A. J.; Lin, C. F.; Noked, M.; Rubloff, G. W. Atomic Layer Deposition of the Solid Electrolyte LiPON. *Chem. Mater.* **2015**, *27*, 5324−5331.

(16) Nisula, M.; Shindo, Y.; Koga, H.; Karppinen, M. Atomic Layer Deposition of Lithium Phosphorus Oxynitride. *Chem. Mater.* **2015**, *27*, 6987−6993.

(17) Su, Y.; Falgenhauer, J.; Polity, A.; Leichtweiß, T.; Kronenberger, A.; Obel, J.; Zhou, S.; Schlettwein, D.; Janek, J.; Meyer, B. K. LiPON Thin Films with High Nitrogen Content for Application in Lithium Batteries and Electrochromic Devices Prepared by RF Magnetron Sputtering. *Solid State Ionics* **2015**, *282*, 63−69.

(18) Yu, X.; Bates, J. B.; Jellison, G. E.; Hart, F. X. A Stable Thin-Film Lithium Electrolyte: Lithium Phosphorus Oxynitride. *J. Electrochem. Soc.* **1997**, *144* (2), 524.

(19) Hamon, Y.; Douard, A.; Sabary, F.; Marcel, C.; Vinatier, P.; Pecquenard, B.; Levasseur, A. Influence of Sputtering Conditions on Ionic Conductivity of LiPON Thin Films. *Solid State Ionics* **2006**, *177*, 257−261.

(20) Suzuki, A.; Sasaki, S.; Murayama, T.; Kimura, I.; Morikawa, Y.; Jimbo, T.; Suu, K. Manufacturing Technology of All-Solid-State Thin-Film Battery for Stand-Alone MEMS/Sensor Application. *TRANSDUCERS 2017 - 19th Int. Conf. Solid-State Sensors, Actuators Microsystems* **2017**, 1871−1874.

(21) Ko, J.; Yoon, Y. S. Effect of Post-Annealing on Structural and Electrochemical Properties of Lithium Phosphorus Oxynitride Thin Film. *Ceram. Int.* **2020**, *46*, 14071−14077.

(22) Westover, A. S.; Dudney, N. J.; Sacci, R. L.; Kalnaus, S. Deposition and Confinement of Li Metal along an Artificial Lipon-Lipon Interface. *ACS Energy Lett.* **2019**, *4*, 651−655.

(23) Fleutot, B.; Pecquenard, B.; Martinez, H.; Letellier, M.; Levasseur, A. Investigation of the Local Structure of LiPON Thin Films to Better Understand the Role of Nitrogen on Their Performance. *Solid State Ionics* **2011**, *186*, 29−36.

(24) Senevirathne, K.; Day, C. S.; Gross, M. D.; Lachgar, A.; Holzwarth, N. A. W. A New Crystalline LiPON Electrolyte: Synthesis, Properties, and Electronic Structure. *Solid State Ionics* **2013**, *233*, 95−101.

(25) Lacivita, V.; Artrith, N.; Ceder, G. Structural and Compositional Factors That Control the Li-Ion Conductivity in LiPON Electrolytes. *Chem. Mater.* **2018**, *30*, 7077−7090.

(26) Suzuki, N.; Shirai, S.; Takahashi, N.; Inaba, T.; Shiga, T. A Lithium Phosphorous Oxynitride (LiPON) Fi Lm Sputtered from Unsintered Li_3PO_4 Powder Target. *Solid State Ionics* **2011**, *191*, 49−54.

(27) Zhao, S.; Fu, Z.; Qin, Q. A Solid-State Electrolyte Lithium Phosphorus Oxynitride Film Prepared by Pulsed Laser Deposition. *Thin Solid Films* **2002**, *415*, 108−113.

(28) Van-Jodin, L. Le; Ducroquet, F.; Sabary, F.; Chevalier, I. Dielectric Properties, Conductivity and Li^+ Ion Motion in LiPON Thin Films. *Solid State Ionics* **2013**, *253*, 151−156.

(29) Chung, K.; Kim, W.; Choi, Y. Lithium Phosphorous Oxynitride as a Passive Layer for Anodes in Lithium Secondary Batteries. *J. Electroanal. Chem.* **2004**, *566*, 263−267.

(30) Schwöbel, A.; Hausbrand, R.; Jaegermann, W. Interface Reactions between LiPON and Lithium Studied by In-Situ X-Ray Photoemission. *Solid State Ionics* **2015**, *273*, 51−54.

(31) Zhao, Q.; Stalin, S.; Zhao, C. Z.; Archer, L. A. Designing Solid-State Electrolytes for Safe, Energy-Dense Batteries. *Nat. Rev. Mater.* **2020**, *5*, 229−252.

(32) Owens, B. B. Solid State Electrolytes: Overview of Materials and Applications during the Last Third of the Twentieth Century. *J. Power Sources* **2000**, *90*, 2−8.

(33) Grady, Z. A.; Wilkinson, C. J.; Randall, C. A.; Mauro, J. C. Emerging Role of Non-Crystalline Electrolytes in Solid-State Battery Research. *Front. Energy Res.* **2020**, DOI: 10.3389/fenrg.2020.00218.

(34) Choi, C. H.; Cho, W. I.; Cho, B. W.; Kim, H. S.; Yoon, Y. S.; Tak, Y. S. Radio-Frequency Magnetron Sputtering Power Effect on the Ionic Conductivities of Lipon Films. *Electrochem. Solid-State Lett.* **2002**, *5*, 14−17.

(35) Thißen, A.; Ensling, D.; Liberatore, M.; Wu, Q. Experimental Routes to in Situ Characterization of the Electronic Structure and Chemical Composition of Cathode Materials for Lithium Ion Batteries during Lithium Intercalation and Deintercalation Using Photoelectron Spectroscopy and Related Techniques. *Ionics* **2009**, *15*, 393−403.

(36) West, W. C.; Hood, Z. D.; Adhikari, S. P.; Liang, C.; Lachgar, A.; Motoyama, M.; Iriyama, Y. Reduction of Charge-Transfer Resistance at the Solid Electrolyte e Electrode Interface by Pulsed Laser Deposition of Films from a Crystalline Li_2PO_2N. *J. Power Sources* **2016**, *312*, 116−122.

(37) Meda, L.; Maxie, E. E. Lipon Thin Films Grown by Plasma-Enhanced Metalorganic Chemical Vapor Deposition in a N_2 - H_2 - Ar Gas Mixture. *Thin Solid Films* **2012**, *520* (6), 1799−1803.

(38) Park, H. Y.; Nam, S. C.; Lim, Y. C.; Choi, K. G.; Lee, K. C.; Park, G. B.; Lee, S.-R.; Kim, H. P.; Cho, S. B.; et al. Effects of Sputtering Pressure on the Characteristics of Lithium Ion Conductive Lithium Phosphorous Oxynitride Thin Film. *J. Electroceram.* **2006**, *17*, 1023−1030.

(39) Nuwayhid, R. B.; Jarry, A.; Rubloff, G. W.; Gregorczyk, K. E. Atomic Layer Deposition of Sodium Phosphorus Oxynitride: A Conformal Solid-State Sodium-Ion Conductor. *ACS Appl. Mater. Interfaces* **2020**, *12*, 21641−21650.

(40) Wang, B.; Chakoumakos, B. C.; Sales, B. C.; Kwak, B. S.; Bates, J. B. Synthesis, Crystal Structure, and Ionic Conductivity of a Polycrystalline Lithium Phosphorus Oxynitride with the γ-Li_3PO_4 Structure. *J. Solid State Chem.* **1995**, *115* (2), 313−323.

(41) Abels, G.; Bardenhagen, I.; Schwenzel, J. One-Pot Synthesis of Polymeric LiPON. *Polymer* **2020**, *192*, 122300.

(42) Mascaraque, N.; Fierro, J. L. G.; Durán, A.; Muñoz, F. An Interpretation for the Increase of Ionic Conductivity by Nitrogen Incorporation in LiPON Oxynitride Glasses. *Solid State Ionics* **2013**, *233*, 73−79.

(43) Lacivita, V.; Westover, A. S.; Kercher, A.; Phillip, N. D.; Yang, G.; Veith, G.; Ceder, G.; Dudney, N. J. Resolving the Amorphous Structure of Lithium Phosphorus Oxynitride (Lipon). *J. Am. Chem. Soc.* **2018**, *140*, 11029−11038.

(44) Dussauze, M.; Kamitsos, E. I.; Johansson, P.; Matic, A.; Varsamis, C. P. E.; Cavagnat, D.; Vinatier, P.; Hamon, Y. Lithium Ion Conducting Boron-Oxynitride Amorphous Thin Films: Synthesis and Molecular Structure by Infrared Spectroscopy and Density Functional Theory Modeling. *J. Phys. Chem. C* **2013**, *117*, 7202−7213.

https://dx.doi.org/10.1021/acs.jpcc.0c10001
J. Phys. Chem. C XXXX, XXX, XXX−XXX

(45) Marple, M. A. T.; Wynn, T. A.; Cheng, D.; Shimizu, R.; Mason, H. E.; Meng, Y. S. Local Structure of Glassy Lithium Phosphorus Oxynitride Thin Films: A Combined Experimental and Ab Initio Approach. *Angew. Chem., Int. Ed.* **2020**, *59*, 22185−22193.

(46) Sicolo, S.; Albe, K. First-Principles Calculations on Structure and Properties of Amorphous $Li_5P_4O_8N_3$(LiPON). *J. Power Sources* **2016**, *331*, 382−390.

(47) Holzwarth, N. A. W. First Principles Modeling of Electrolyte Materials in All-Solid-State Batteries. *Phys. Procedia* **2014**, *57*, 29−37.

(48) Le Van-Jodin, L.; Ducroquet, F.; Sabary, F.; Chevalier, I. Dielectric Properties, Conductivity and Li^+ Ion Motion in LiPON Thin Films. *Solid State Ionics* **2013**, *253*, 151−156.

(49) Sushko, M. L.; Rosso, K. M.; Zhang, J. G.; Liu, J. Multiscale Simulations of Li Ion Conductivity in Solid Electrolyte. *J. Phys. Chem. Lett.* **2011**, *2*, 2352−2356.

(50) Put, B.; Vereecken, P. M.; Stesmans, A. On the Chemistry and Electrochemistry of LiPON Breakdown. *J. Mater. Chem. A* **2018**, *6*, 4848−4859.

(51) Richards, W. D.; Miara, L. J.; Wang, Y.; Kim, J. C.; Ceder, G. Interface Stability in Solid-State Batteries. *Chem. Mater.* **2016**, *28*, 266−273.

(52) Zhu, Y.; He, X.; Mo, Y. Origin of Outstanding Stability in the Lithium Solid Electrolyte Materials: Insights from Thermodynamic Analyses Based on First-Principles Calculations. *ACS Appl. Mater. Interfaces* **2015**, *7*, 23685−23693.

(53) Wang, Z.; Santhanagopalan, D.; Zhang, W.; Wang, F.; Xin, H. L.; He, K.; Li, J.; Dudney, N.; Meng, Y. S. In Situ STEM-EELS Observation of Nanoscale Interfacial Phenomena in All-Solid-State Batteries. *Nano Lett.* **2016**, *16*, 3760−3767.

(54) Santhanagopalan, D.; Qian, D.; McGilvray, T.; Wang, Z.; Wang, F.; Camino, F.; Graetz, J.; Dudney, N.; Meng, Y. S. Interface Limited Lithium Transport in Solid-State Batteries. *J. Phys. Chem. Lett.* **2014**, *5*, 298−303.

(55) Fingerle, M.; Buchheit, R.; Sicolo, S.; Albe, K.; Hausbrand, R. Reaction and Space Charge Layer Formation at the LiCoO2-LiPON Interface: Insights on Defect Formation and Ion Energy Level Alignment by a Combined Surface Science-Simulation Approach. *Chem. Mater.* **2017**, *29*, 7675−7685.

(56) Jacke, S.; Song, J.; Cherkashinin, G.; Dimesso, L.; Jaegermann, W. Investigation of the Solid-State Electrolyte/Cathode LiPON/$LiCoO_2$ Interface by Photoelectron Spectroscopy. *Ionics* **2010**, *16*, 769−775.

(57) Leung, K.; Pearse, A. J.; Talin, A. A.; Fuller, E. J.; Rubloff, G. W.; Modine, N. A. Kinetics-Controlled Degradation Reactions at Crystalline LiPON/Li_xCoO_2 and Crystalline LiPON/Li-Metal Interfaces. *ChemSusChem* **2018**, *11*, 1956−1969.

(58) Kim, Y. G.; Wadley, H. N. G. Lithium Phosphorous Oxynitride Films Synthesized by a Plasma-Assisted Directed Vapor Deposition Approach Lithium Phosphorous Oxynitride Films Synthesized by a Plasma-Assisted Directed Vapor Deposition Approach. *J. Vac. Sci. Technol., A* **2008**, *26*, 174.

(59) Takada, K. Progress in Solid Electrolytes toward Realizing Solid-State Lithium Batteries. *J. Power Sources* **2018**, *394*, 74−85.

(60) Li, D.; Ma, Z.; Xu, J.; Li, Y.; Xie, K. High Temperature Property of All-Solid-State Thin Film Lithium Battery Using LiPON Electrolyte. *Mater. Lett.* **2014**, *134*, 237−239.

(61) Yu, X.; Bates, J. B.; Jellison, G. E.; Hart, F. X. A Stable Thin - Film Lithium Electrolyte: Lithium Phosphorus Oxynitride A Stable Thin-Film Lithium Electrolyte: Lithium Phosphorus Oxynitride. *J. Electrochem. Soc.* **1997**, *144*, 524.

(62) Belous, A. G.; V, O. I.; Kovalenko, L. L.; Bohnke, O.; Bohnke, C. Synthesis of Thin Film Electrodes Based on LiPON and LiPON - LLTO - LiPON. *Russ. J. Electrochem.* **2014**, *50*, 523−530.

(63) Lapp, T.; Skaarup, S.; Hooper, A. Ionic Conductivity of Pure and Doped Li_3N. *Solid State Ionics* **1983**, *11*, 97−103.

(64) Nazri, G. Preparation, Structure and Ionic Conductivity of Lithium Phosphide. *Solid State Ionics* **1989**, *34*, 97−102.

(65) Cheng, D.; Wynn, T. A.; Wang, X.; Wang, S.; Zhang, M.; Shimizu, R.; Bai, S.; Nguyen, H.; Fang, C.; Kim, M. cheol; et al. Unveiling the Stable Nature of the Solid Electrolyte Interphase between Lithium Metal and LiPON via Cryogenic Electron Microscopy. *Joule* **2020**, *4*, 2484−2500.

(66) LaCoste, J.; Li, Z.; Yun, X.; He, Z.; Matherne, D.; Zakutayev, A.; Fei, L. Investigating the Effects of Lithium Phosphorous Oxynitride Lamination on PEO/PPC Blended Hybrid Electrolytes. *ACS Appl. Mater. Interfaces* **2020**, *12*, 40749−40758.

(67) Ko, J.; Yoon, Y. S. Data on the Observation of the Interface between Lithium Phosphorus Oxynitride Film and Lithium Layer. *Data Br.* **2020**, *33*, 106612.

(68) Nimisha, C. S.; Rao, G. M.; Munichandraiah, N.; Natarajan, G.; Cameron, D. C. Chemical and Microstructural Modifications in LiPON Thin Films Exposed to Atmospheric Humidity. *Solid State Ionics* **2011**, *185*, 47−51.

(69) Han, F.; Westover, A. S.; Yue, J.; Fan, X.; Wang, F.; Chi, M.; Leonard, D. N.; Dudney, N. J.; Wang, H.; Wang, C. High Electronic Conductivity as the Origin of Lithium Dendrite Formation within Solid Electrolytes. *Nat. Energy* **2019**, *4*, 187−196.

(70) Weiss, M.; Seidlhofer, B. K.; Geiß, M.; Geis, C.; Busche, M. R.; Becker, M.; Vargas-Barbosa, N. M.; Silvi, L.; Zeier, W. G.; Schröder, D.; et al. Unraveling the Formation Mechanism of Solid-Liquid Electrolyte Interphases on LiPON Thin Films. *ACS Appl. Mater. Interfaces* **2019**, *11*, 9539−9547.

(71) Kanazawa, S.; Baba, T.; Yoneda, K.; Mizuhata, M.; Kanno, I. Deposition and Performance of All Solid-State Thin-Film Lithium-Ion Batteries Composed of Amorphous Si/LiPON/VO-LiPO Multilayers. *Thin Solid Films* **2020**, *697*, 137840.

(72) Wang, C.; Bai, G.; Yang, Y.; Liu, X.; Shao, H. Dendrite-Free All-Solid-State Lithium Batteries with Lithium Phosphorous Oxynitride-Modified Lithium Metal Anode and Composite Solid Electrolytes. *Nano Res.* **2019**, *12*, 217−223.

(73) Wang, W.; Yue, X.; Meng, J.; Wang, J.; Wang, X.; Chen, H.; Shi, D.; Fu, J.; Zhou, Y.; Chen, J.; et al. Lithium Phosphorus Oxynitride as an Efficient Protective Layer on Lithium Metal Anodes for Advanced Lithium-Sulfur Batteries. *Energy Storage Mater.* **2019**, *18*, 414−422.

(74) Tenhaeff, W. E.; Yu, X.; Hong, K.; Perry, K. A.; Dudney, N. J. Ionic Transport across Interfaces of Solid Glass and Polymer Electrolytes for Lithium Ion Batteries. *J. Electrochem. Soc.* **2011**, *158*, A1143−A1149.

(75) Uitz, M.; Epp, V.; Bottke, P.; Wilkening, M. Ion Dynamics in Solid Electrolytes for Lithium Batteries Probing Jump Rates and Activation Energies through Time-Domain Li NMR. *J. Electroceram.* **2017**, *38*, 142−156.

(76) Fu, Z.; Liu, W.; Li, C.; Qin, Q.; Yao, Y.; Lu, F.; Fu, Z.; Liu, W.; Li, C.; Qin, Q. High-k Lithium Phosphorous Oxynitride Thin Films. *Appl. Phys. Lett.* **2003**, *83*, 5008.

(77) Liu, Y.; Xie, K.; Pan, Y.; Wang, H.; Chen, Y.; Li, Y.; Zheng, C. Impacts of the Properties of Anode Solid Electrolyte Interface on the Storage Life of Li-Ion Batteries. *J. Phys. Chem. C* **2018**, *122*, 9411−9416.

(78) Lin, C. F.; Fan, X.; Pearse, A.; Liou, S. C.; Gregorczyk, K.; Leskes, M.; Wang, C.; Lee, S. B.; Rubloff, G. W.; Noked, M. Highly Reversible Conversion-Type FeOF Composite Electrode with Extended Lithium Insertion by Atomic Layer Deposition LiPON Protection. *Chem. Mater.* **2017**, *29*, 8780−8791.

https://dx.doi.org/10.1021/acs.jpcc.0c10001
J. Phys. Chem. C XXXX, XXX, XXX−XXX